Aalto University Publications in Materials Science and Engineering
Aalto-yliopiston materiaalitekniikan julkaisuja
Espoo 2010 TKK-MT-214

Sulfide Mineralogy - Literature Review

F. Tesfaye Firdu, P. Taskinen

Aalto-yliopisto Teknillinen korkeakoulu
Aalto-universitetet Tekniska högskolan
Aalto University School of Science and Technology

Aalto University Publications in Materials Science and Engineering
Aalto-yliopiston materiaalitekniikan julkaisuja
Espoo 2010 TKK-MT-214

Sulfide Mineralogy - Literature Review

F. Tesfaye Firdu, P. Taskinen

Aalto University School of Science and Technology
Department of Materials Science and Engineering
Thermodynamics and Modeling of Metallurgical Processes (TDM)

Aalto-Yliopiston Teknillinen korkeakoulu
Materiaalitekniikan Laitos
Metallurgisten Prosessien Termodynamiikka ja Mallinnus (TDM)

Research program: ELEMET (Energy & Lifecycle Efficient Metal Processes)
Project: ISS (Improved Sulfide Smelting)
Financers: Boliden Harjavalta Oy, Boliden Kokkola Oy, Norilsk Nickel Finland Oy, Outotec Oyj and the Finnish Funding Agency for Technology and Innovation (Tekes)
Keywords: Fe-S, Ni-S, Cu-S, Zn-S, Phase equilibrium, Thermodynamics

Distribution:
Aalto University School of Science and Technology
Department of Materials Science and Engineering
P.O. Box 16200
FI-00076 Aalto, Finland
Tel. +358 9 470 22796
Fax. +358 9 470 22798
E-mail: Fiseha.Tesfaye@tkk.fi

ISBN 978-952-60-3271-9
ISSN 1455-2329

Multiprint Oy
Espoo 2010

Abstract

The aim of this study was to have an insight into the sulfide mineralogy, mainly based on a book [1] that contains most of the sulfides mineralogical studies prior to the year 1975. In the first two chapters, the metal sulfides crystal structures and chemistries are reviewed. Then, the electronic interactions and chemical bonding followed by experimental methods in sulfides research with the proposed phase equilibria are reviewed. The (Cu, Ni, Zn)-S systems are virtually discussed. Due to its influential and common appearance, in most natural sulfides (the common rock-forming minerals: po and py), the Fe-S system is summarized relatively in detail. Finally, the sulfide petrology is lightly discussed.

The metal sulfides are the raw materials for most of the world supplies of non-ferrous metals. Their complex chemistry, as a result of high impurities association (such as; As, Sb, Bi, etc...) and less base-metals content (metal poor rocks: $X_{(base\text{-}metal)} < 1$ %), and the ever growing demand for the metals as well as the embroiling need to optimize minerals processing and sulfides smelting claim intense mineralogical studies. The main goal of such studies are to acquire accurate thermodynamic data which are useful to predict reactions and stable relationships, and in defining the limiting conditions under which phases may exist.

Table of Contents

Symbols, Abbreviations, Units

a_{S_2}	*activity of sulfur*
al	*anilite (Cu_7S_5)*
bn	*bornite (Cu_5FeS_4)*
bcv	*"blue remaining"covelite (CuS)*
X	*bulk composition*
cc	*chalcocite (Cu_2S)*
cv	*covelite (CuS)*
dg	*digenite (Cu_9S_5)*
dj	*djurleite ($Cu_{1.96}S$)*
fcc	*face centered cubic*
f_{S_2}	*fugacity of sulfur*
hcp	*hexagonal close packed*
iss	*intermediate solid solution*
L	*liquid*
T_m	*melting temperature (^oC)*
M	*metal*
M-M	*metal-metal bonding*
M-S	*metal-sulfur bonding*
mss	*monosulfide solid solution*
M_9S_8	*pentlandite (M=Fe, Co, Ni)*
P	*pressure (atm)*
pc	*primitive cubic*
py	*pyrite (FeS_2)*
po	*pyrrhotite ($Fe_{1-x}S$ (x = 0…0.2))*
S-S	*sulfur-sulfur boding*
T	*temperature (^oC)*
tr	*troilite (FeS)*

1 Introduction

The metallic sulfide minerals have been known and valued as sources of metals from the earliest times. Most of them are crystalline solids. They are the most important group of ore minerals, constituting the raw materials for most of the world supplies of non-ferrous metals. Synthetic studies of their phase equilibria began in metallurgical laboratories in the late nineteenth and early twentieth centuries. These were generally confined to the M-rich portions of the M-S systems analogous to the smelter products, but were applicable to the ore mineralogy of some magnetic deposits of low sulfur content. Sulfides research was severely limited by the times available techniques (reflected-light microscopy, etching and wet microchemical methods) for analyzing the experimental products until the introduction of X-ray diffraction in the 1920s.

Subsequently, research activities were particularly stimulated by the work of Kullerud et al. [2] on the FeS-ZnS system, which suggested the possibility of sulfide geothermometry, and by the thermochemical studies of Rosenqvist et al. [3]. Since then, the phase equilibria of nearly every binary sulfide, selenid and telluride system and many of the ternary and quaternary systems have been investigated. Detailed thermochemical studies such as the work of Toulmin et al. [4] on the Fe - S system have permitted sulfide systems of increasing complexity to be somehow understood.

The study of phase equilibria involves the physical relationships among either natural or synthetic materials. Different ways of sulfide experiments using the evacuated silica tube method has been developed. The objectives of such studies are the determination of the coexistence of phases at equilibrium and the interdependence of thermal stability, pressure stability, vapor pressure and activity of phases. Different techniques such as microscopy and X-ray diffractometery are employed to determine the phase equilibria.

Studies of phase equilibria contributed significantly to our understanding of the conditions of mineral genesis and post-depositional alteration. Processes involved in the minerals beneficiation and refining, the distribution of elements between minerals and the conditions under which various sulfide phases may exist, have been clarified. The prediction of several sulfide minerals before their discovery has also been possible.

2 Determination, Relationships and Classification of Sulfide Mineral Structures

Experimental difficulties to determine the sulfides crystal structure make their study amenable than any other inorganic compounds. The acquisition of detailed structural information has therefore lagged in comparison to the other magnetic materials. The gaps in the understanding of the sulfides crystal chemistry partly stems out of the lack of data, as well as the complexity of these minerals. Unlike other minerals, sulfides are often massive and poorly crystallized. Crystals of some species are almost invariably bent or posses low-angle grain boundaries. Certain sulfides and sulfosalts have pronounced a circular habit, occurring only as bundles of fibers which have their axes of elongation in common.

Close-packed arrays of sulfur atoms form the basic structure of many simple sulfides. Small displacement of the metal atom positions often causes the true symmetry of the structure to be lower than that of the ideal close-packed array. These structures are pseoudosymmetric and thus are commonly and sometimes invariably twined. Monoclinic pyrrhotite (Fe_7S_8) for example, is markedly pseudo-hexagonal. According to Wuensch et al. [1], a single only untwined fragment has never been discovered. The problem of twining is compounded if, in addition to being pseudosymmetric, the mineral displays a rapid phase transformation to a more symmetric form at a temperature which is lower than that of deposition. For example, chalcocite (Cu_2S), which is monoclinic at low temperatures [5], transforms to a hexagonal form at ~105^{o}C. The low temperature form, usually twinned, was thought to be orthorhombic and pseudo-hexagonal. Twining need not prevent a crystal structure determination. The X-ray intensities which were measured may be proportioned to the separate members of a twin provided that the members are of unequal volume or if not all reflections superposes. Such analysis requires the collection of much redundant data and is too tedious to apply.

One of the problems in isolating the suitable specimen is exsolution following the deposition. The presence of the second phase may be difficult to detect if the intergrowth is coherent. More insidious types of intergrowths are known in sulfides. For example, a large number of phases with slightly different (Pb + Cu): Bi ratios appear to exist as superstructures intermediate to aikinite ($PbCuBiS_3$) and bismuthinite (Bi_2S_3). Coherent intergrowths of several of these phases have been observed [6].

Most of the natural minerals exhibit solid solutions. In primarily ionic materials the extent to which solid solution occurs is determined by the radius of the ions involved and the ions charge balance. Sulfides and sulfosalts have predominantly covalent or metallic character. Difficulty to determine the extent of solid solutions in sulfides and sulfosalts are manifested by many researchers. For example, tetrahedrite (Cu_3SbS_3 or Cu_3SbS_{3+x}) was shown by Pauling et al. [7] and Wuensch et al. [1], through structural determination, to have the unlikely composition $Cu_{12}Sb_4S_{13}$. However, Skinner et al. [8] and Tatsuka et al. [9] have shown a wide solid solution range;

$Cu_{12+x}Sb_{4+y}S_{13}$ with $0.11 < x < 1.77$ and $0.03 < y < 0.3$, the stability field in which neither of the above structures ((Cu_3SbS_3 or Cu_3SbS_{3+x}), $Cu_{12}Sb_4S_{13}$) exist. In sulfides even small amounts of impurities are often problematic, however, the mechanism and effect of them was not fully understood until the 1970s.

The sulfide systems are susceptible to polymorphism. Sphalerite/wurtzite and marcasite/pyrite are good examples of sulfide polymorphs. Since, the atomic arrangements are distinct, their energies cannot be precisely the same, however close, which implies that at a given temperature and pressure only one polymorph structure is stable.

3 Sulfides Crystal Chemistry

The ability of sulfur to form covalent bonds is reflected in the ease with which repeated S-S bonds may form to create chains or rings. This ability has no counterpart in oxide or silicate mineralogy. One example is provided by polysulfide ion; S_n^{2-}, where n = 2…6. The thionate ions, $S_nO_6^{2-}$, have analogous structure but terminate with a pyramid of oxygen atoms. Sulfur forms pure ionic bonds only with the very electropositive ions of low valence, sulfide of group II are a good examples of the ionic sulfides.

The stability of sulfur at normal temperature and pressure is orthorhombic, as illustrated in Figure 1. A rhombohedral form of sulfur may be crystallized from solutions. Through the crystallization Donohue et al. [10] observed S_6 molecules, as shown in Figure 1 (b).

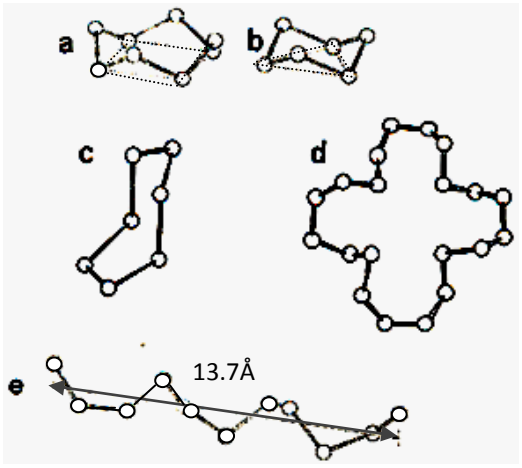

Figure 1. Atomic arrangements in polymorphs of elemental sulfur a) S_8 ring found in α, β and γ sulfur b) S_6 ring in rhombohedral sulfur c) S_7 d) S_{20} e) helical chain found in fibrous forms of sulfur.

In most sulfosalts the Group V metal forms either three nearly orthogonal bonds or, alternatively, a [1 + 2 + 2] square pyramidal coordination with sp^3d^2 hybridation. Many sulfosalts are therefore derived from the sphalerite structure (Appendix A) by omission of the fourth S atom which would have been bonded to the Group V metals. Marumo's et al. [11] work on rhombohedral mineral, nowakilt ($Cu_6Zn_3As_4S_{12}$) is a good example.

The Nickel-Arsenide (NiAs) structure (shown in appendix A) type is assumed by most of the transition metal sulfides. It is a hexagonal structure in which the more electronegative atoms are arranged in hcp. Nonstoichiometry (usually metal atom vacancies) and derivative structure are very common. Pyrrhotite ($Fe_{1-x}S$), which is important in rock-forming mineralogy, is an extremely complex derivative of the NiAs structure type. Troilite, stoichiometric FeS, has a structure derivative of NiAs through small displacements of S parallel to c [12]. According to Hall et al. [13], the structure of argentian pentlandite ($(Fe,Ni)_8AgS_8$) has been refined, and the octahedral sites were

found to be occupied exclusively by the Ag atoms. The crystal structure of the copper sulfide system is discussed in section 6.1.2.1.

Certain trends are becoming clear in the crystal chemistry of the Pb-Cu-Bi sulfides. If the lead content of the mineral is high, the structure assumed is a “composite” structure based on PbS-like domains. Studies of Takagi et al. [14] on lillianite ($Pb_3Bi_2S_6$) and Weitz et al. [15] on cosalite ($Pb_2Bi_2S_5$) are good examples. If a mineral contains no lead, or if the ratio of Bi and Cu to Pb is high, the structure contains chain-like units. When the copper content is high, a network of copper tetrahedra or triangles like Bi-containing chains together, and forms an important feature of the structure. According to Kupcik et al. [16], this occurs in emplectite ($CuBiS_2$), hodrushite ($PbCu_4Bi_5S_{11}$) and $Cu_4Bi_5S_9$. On the other hand, if the Cu content is relatively low, the copper atoms play a passive role in the structure and occupy interstices between bismuthinite or emplectite-like chains. This occurs in ($CuBi_5S_8$) [17] and aikinite ($PbCuBiS_3$) and gladite ($PbCuBi_5S_9$) [18]. According to Kohatsu et al. [19], nuffieldite ($Pb_2Cu(Pb,Bi)Bi_2S_7$) contains a complex 10-membered ribbon.

4 Electron Interactions and Chemical Bonding in Sulfides

The transition metals, characterized by the presence of unpaired electrons, are crucial in understanding sulfide chemistry. The ions of the first raw transition elements are listed in Table 1.

Structural studies on the (Fe, Co, Ni)-S minerals revealed the fact that their structures contain short M-M distances, which suggested the presence of metallic bonds [20, 21, 22, 23, 24, 25]. Although these M-M bonds could account for the metallic properties, the reasons for the formation of such bonds and their influence on the cation-anion bonding were not well understood. These authors suggested that the phases are stabilized by M-M bonds which apparently control the solid solution behavior of these structures. The observed bond lengths and the number of bonds in each structure are listed in Table 2.

Table 1. The first row transition elements and ions. Oxidation state corresponding to the underlined entries [20].

	d^0	d^1	d^2	d^3	d^4	d^5	d^6	d^7	d^8	d^9	d^{10}
0^+		Sc	Ti	V		Cr/Mn	**Fe**	**Co**	**Ni**		**Cu**/Zn
1^+							Mn			Ni	**Cu**
2^+			Ti	V	**Cr**	**Mn**	**Fe**	**Co**	**Ni**	**Cu**	**Zn**
3^+	**Cs**	**Ti**	**V**	**Cr**	**Mn**	**Fe**	**Co**	Ni	Cu		**Ga**
4^+	**Ti**	**V**	Cr	**Mn**	Fe	Co	Ni				**Ge**
5^+	**V**	Cr	Mn								**As**
6^+	**Cr**	Mn	Fe								**Se**
7^+	Mn										Br

Table 2. M-M/S coordination and M-S distances in selected sulfides [20, 23, 24, 25].

Name	Composition	M-S Coordination	M-M Coordination	M-S Distance, Å
Mackinawite	$Fe_{1+x}S$	4	4	2.602
Co-pentlandite	Co_9S_8	6, 4	3	2.505
Pentlandite	$(Fe,Ni,Co)_9S_8$	6,4	3	2.531
Millerite	NiS	5	2	2.534
Heazlewoodite	Ni_3S_2	4	4?	2.49
αNi_7S_6	Ni_7S_6	5, 4	2?	2.492

The aftermath studies suggested that the M-M interactions affect the cation-anion distances. However, the correction factor for the metal interaction, which affected the cation-anion distances, is not known.

4.1 Application of Bonding Theory

To illustrate how molecular orbital and bond theories are used to help our understanding of bonding and solid solution behavior of the transition metal ions in sulfide minerals Rajamani et al. [20] has chosen pyrite, thiospinels and pentlandite. The structure of pyrite (in which no direct or

indirect metal interaction occurs) is based on an fcc array of ions with NaCl-type structure. The M-S distance of the pyrite, as shown in Table 3, is relatively shorter than the theoretical distance, 2.62Å, obtained by adding the radii of $^{VI}Fe^{2+}$ and $^{IV}S^{2-}$. This indicates that the Fe-S bonding in FeS_2 is essentially covalent.

Table 3. Inter atomic distances in the transition metal disulfides [20].

	FeS_2	CoS_2	NiS_2	CuS_2
M^{2+}-S distance(Å)	2.26	2.34	2.40	-

The limits of solid solution in the ternary system FeS_2-CoS_2-NiS_2, shown in Figure 2 (a), can also be explained by the scheme given in Table 3. Incompleteness of the solid solution between FeS_2 and NiS_2 (as shown in Figure 2) could attribute to the intra-atomic distances given in Table 3.

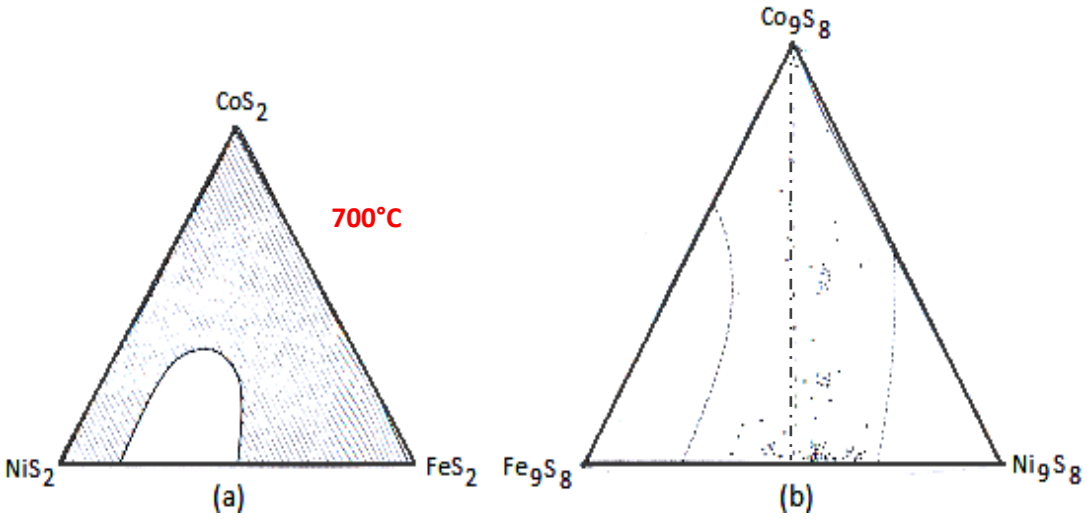

Figure 2. a) Solid solution in the FeS_2-CoS_2-NiS_2 system at 700°C [26]. b) Natural pentlandite composition [22]. Dashed lines represent the estimated solid-solution in the M_9S_8 section of the Fe-Co-Ni-S system as limits out-lined by Knop et al. [27]. Dashed-dot line represents compositions for which Fe:Ni = 1.

Common sulfide minerals with the spinel structure (e.g $CuCo_2S_4$, Co_3S_4, $[(Co,Ni)_3S_4]$, Ni_3S_4), which is based on the cubic close packing of sulfur atoms, exhibit indirect M-M interactions [28]. Pentlandite, which occasionally contains Ag (up to 10 wt. %), has a structure based on the pseudo-cubic closest packing of sulfur atoms. The interatomic distances and magnetic and electrical properties in pentlandite suggest the presence of extensive M-S covalent bonding and M-M interaction in the structure. The cube-cluster of metal atoms in the pentlandite structure has an important effect on the chemistry of this mineral. Of the three possible end members (Fe_9S_8, Co_9S_8 and Ni_9S_8) Co_9S_8 was observed to form a stable homogenous phase in the Fe-Co-Ni-S system [27].

Natural pentalndite have also a restricted range in composition as shown in Figure 2 (b). Increasing the Ni content in the pentlandite over the ratio Ni:Fe $\geq$ 1 will increase the number of d electrons in the unit cell. Ordering of Ni in the octahedral site and creation of cation vacancies in the tetrahedral sites could effectively keep the number of d electrons at a constant value. Similarly, because Fe has only six 3d electrons, increasing the Fe content in pentlandite over the ratio Ni:Fe $\geq$ 1 will result in the addition of excess cations in the unoccupied tetrahedral sites to maintain a constant number of electrons, as in an electron compound (where the ratio of electrons to atoms is fixed). Therefore, the structural formula for pentlandite could be [Fe, Co, Ni](Fe, Co, Ni, Va)$_8$S$_8$, where Va represents tetrahedral vacancies in Ni-rich compositions or excess cations in Fe-rich compositions. Thus, the nonstoichiometry of pentlandites is due to metal addition and omission of the solid solution.

5 Experimental Methods in Sulfide Synthesis

Advances in the sulfide research enabled the simultaneous study of structures as well as determination of phase relations and the underlying thermodynamics. Construction of a phase diagram requires the location of all phase boundaries for the system chosen; that is, the determination of which phases are in equilibrium at a particular T, P and X. All or part of the P-T-X conditions under study might be outside of those found in nature or, conversely, some compounds have been synthesized before they were found as minerals.

Hypothesis for testing equilibrium state in experimental studies, as stated by Scott et al. [1], can be summarized as follows: a system is held at constant conditions and the products are examined periodically. After initial reaction, if no further changes are noted, eventually, and the same result is achieved for experiments with different initial conditions, then the system is assumed to have reached equilibrium. However, this kind of test cannot be completely reliable.

The best test for equilibrium state is to disturb the system in some manner causing change in the phases and then return the system to its original conditions. If the phases retain their original states, the reaction is said to have been reversed and equilibrium is assumed [29]. However, one possible source of error for correct interpretation of the experimental results is the formation of metastable phases and failure to recognize them, especially when the activation energy barrier between the metastable and equilibrium states is large. That means the system survives the test of reversibility and so undetected. The real difficulties are encountered when complete reaction occurs outside the stable phase field of an assemblage. A good example of this was observed in the results obtained by Taylor et al. [30] and Kissin et al. [31]. Taylor et al. [30] was able to reverse the metastable reaction: monoclinic pyrrhotite ⇌ hexagonal pyrhotite at 292^{o}C (solid state reaction); whereas Kissin et al. [31], using hydrothermal technique to flux the reaction, found that monoclinic pyrrhotite inverted reversibility to hexagonal pyrrhotite + pyrite at 254^{o}C.

Experimental studies of sulfides involve synthesis and analysis of the synthesized sulfides at different conditions. Synthesis of sulfide through the dry reaction in an evacuated silica tube is a time-honored process, which is widely used than any other method. One of the most important reasons to choose silica tube in sulfides experiments is because it neither devitrifies, below 1100^{o}C, nor reacts with sulfur.

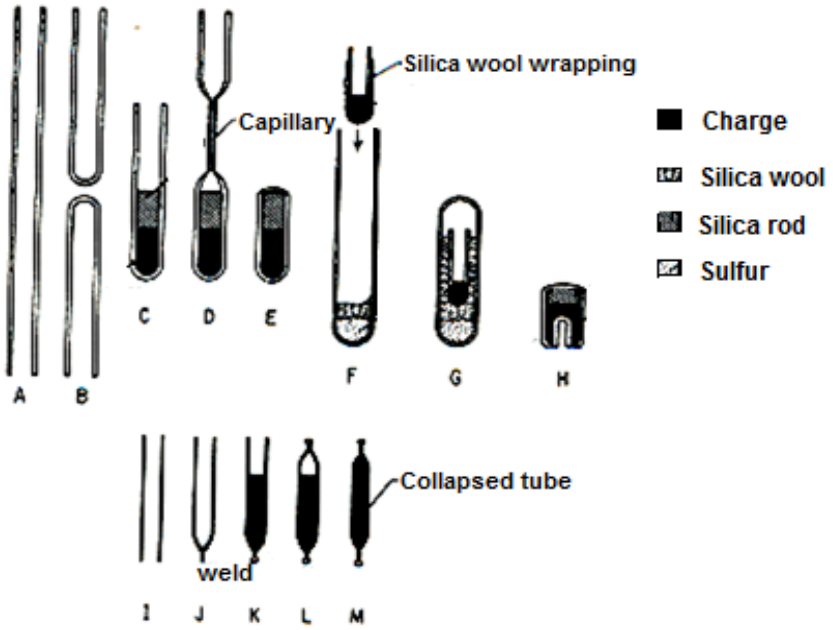

Figure 3. Various types of tubes used in sulfide experiments: A-E, simple evacuated silica tube with a glass rod; F-G, tube-in-tube; H, diffraction thermal analysis; I-M, collapsible precious metal tube [32].

Furthermore, a thin enough silica tube is somewhat transparent to X-rays so it is possible to follow reactions in a high temperature X-ray camera by sealing sulfides into a capillary [33]. The preparation of a standard evacuated silica-tube experiment is illustrated in Figure 3 above.

The charges sealed in to evacuated silica tubes are placed in furnaces to promote reactions at selected temperature. To avoid explosion of the tubes (if thin-walled) at about ~445^{o}C (boiling point of sulfur), the charges should be preheated below 600^{o}C to combine sulfur and metals before attaining the desired run temperature. One of the advantages of using the evacuated silica tube method is that synthesized products can be quenched rapidly by plunging the tubes into water, which is important future in the sulfide experiments. However, there are also some limitations like:

- Solid-state diffusion rate in some sulfides make difficult to attain equilibrium in a reasonable time range and metastability is frequently encountered.
- Obtained products are usually too fine grained to conduct the single-crystal X-ray diffractometry.
- Activity of sulfur cannot be varied at will.

Differential thermal analysis (DTA), which uses temperature variations while phase changes, has an advantage of showing the speed with which the phase boundaries change can be detected compared with appearance-of-phase experiments. However, heat effect by itself does not tell phases consumed or produced. Thus, the result can be interpreted only by the prior knowledge of the phase relations under investigation.

To alter the reaction kinetics in the evacuated silica tube experiments; fluxes (Table 4) or catalysts, in which sulfides are only slightly soluble, are added to the charges to increase reactivity among the sulfides without shifting their equilibrium temperatures. In addition to speeding up the sulfide reactions, the salt fluxes could coarsen run products.

Table 4. Binary salt fluxes used by Moh et al. [33] for sulfide phase equilibrium experiments.

Salt	Mole Ratio	Temperature (^{o}C)
NaCl-KCl	50:50	> 675
KCl-LiCl	42:58	> 360
NH_4Cl-LiCl	<50:50	270-350
KCl-$AlCl_3$	34:66	> 130

Hydrothermal recrystallization method permits large single crystal formation and independent variation of pressure, as described by Barnes et al. [34]. In this method aqueous solutions, in which the sulfides are slightly soluble, are used to promote crystal growth. Figure 4 shows the two procedures used for this method.

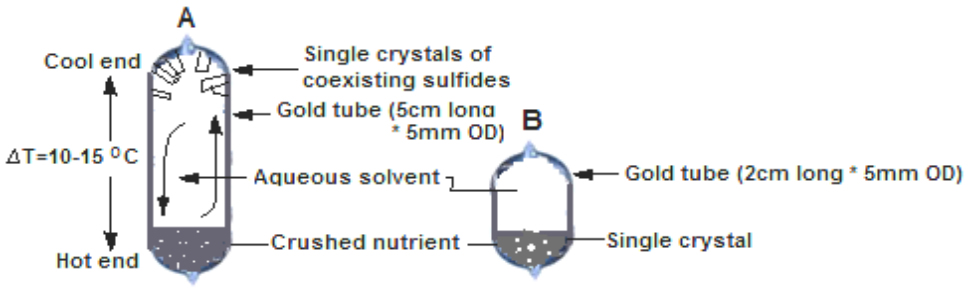

Figure 4. Design for Hydrothermal recrystallization experiments [34]: (A) temperature gradient (which should be as small as 10 - 15^{o}C); (B) *in situ*.

The nutrient material should preferably be finely crushed metallic sulfides rather than a mixture of the native elements. This is because to avoid zoning of M-rich parts in the crystals to be grown.

Criteria for choosing the aqueous solutions:

- Must be stable at the pressure and temperature of the experiment.
- The sulfide mineral subject for synthesis must be stable within the range of fo_2, f_{S_2} and pH provided by the solution.
- Provides good solubility of sulfide minerals and favors diffusion or mass transfer for the crystals to grow.
- The aqueous solute anions must not be soluble in the sulfide. For example, ionic radius of I^- (2.16 Å) differs more from S^{2-}(1.84 Å) than does Cl^- (1.81 Å), thus iodide solutions are less likely to contaminate sulfides than are chloride solutions.

An important advantage of the hydrothermal recrystallization technique is that the aqueous phase can, under certain conditions, provide step less control for fo_2, f_{S_2} and pH over a wide range of values. These variables, which are dependent on each other, along with temperature and to some extent pressure, are the most important factors governing stability and solubility of sulfide minerals [35]. For example, Kissin et al. [36] controlled f_{S_2} by buffering f_{O_2} near the $(SO_4)^{2-}$/HS boundary via the reaction $HS^- + 2O_2 \rightleftharpoons (SO_4)^{2-} + H^+$ and by varying pH with different concentration of NaOH solutions. In their experiments the NaOH solution had two roles; it was the growth medium for large zinc sulfide single crystals and it established on f_{S_2} at each temperature.

Analyses of the obtained products are done by the microscope, X-ray diffraction, microprobe analysis, etc… A microscope is an indispensable tool for examination. Using X-ray difractometry some of the run products' composition can be measured in addition to the phase identifications. However, X-ray diffractometry requires a phase presence of at least 10 - 15 % in a mixture for reliable identification.

Chemical analysis *in situ* can be performed by three techniques of microprobe analysis, these are; electron probe micro analysis, laser microprobe and ion microprobe. The electron microprobe is, as the X-ray diffractometry, a nondestructive analysis and it covers very small areas ideally suited to check homogeneity and determining compositions of fine-grained products or intricate inter growth provided that, as a rule of thumb, the area to be analyzed should be 2.5 times the beam diameter (3 - 5µm routinely). The laser microprobe, though expensive, has a chief advantage (in sulfide research) over the electron microprobe in that, it is possible to measure traces as well as minor and major elements and to discriminate isotopes *in situ*. Results of the experiments can be presented diagrammatically in a number of ways depending on the variables measured. The most commonly used are T - X and $\log as_2$-10^3/T plots.

6 Measurement of Sulfur Activity

Many sulfide equilibria can be represented by sulfidation reactions of the type

$$2M_xS_y\,(s) + S_2 \rightleftharpoons 2M_xS_{y+1}\,(s) \qquad (1)$$

where x= 1,2,3… , and y= 0,1,2… If the solids are in their standard states, their activity will be unity and the equilibrium constant, K, for the reaction is only a function of temperature and activity (or fugacity) of S_2(g):

$$\mathrm{K} = \mathrm{a}_{\mathrm{S}_2}^{-1} = \mathrm{f}_{\mathrm{S}_2}^{-1} \text{ (a standard state fugacity at 1 atm)} \qquad (2)$$

Its variation with temperature, at constant pressure, is given by the Van't Hoff's expression as follows:

$$\frac{\mathrm{d}(\log \mathrm{K})}{\mathrm{d}(1/\mathrm{T})} = \frac{\Delta \mathrm{H}^{\mathrm{o}}}{2.303\mathrm{R}} = \frac{\mathrm{d}(\log \mathrm{a}_{\mathrm{S}_2})}{\mathrm{d}(1/\mathrm{T})} \qquad (3)$$

where ΔH^o is the standard enthalpy of the reaction and R is the universal gas constant. Thus, plots of $loga_{S_2}$ against 1/T for a sulfidation reaction is linear with a slope of $\frac{\Delta H^o}{2.303R}$. If one or both of the solid phases are not in their standard states the sulfidation reaction will represent a curved line. This is due to consideration of the activities of both the solids and the partial pressure of the gas in the equilibrium expression, i.e:

$$\frac{\mathrm{d}(\log \mathrm{a}_{\mathrm{S}_2})}{\mathrm{d}(1/\mathrm{T})} = \frac{\Delta \mathrm{H}^{\mathrm{o}}}{2.303\mathrm{R}} \cdot \pi_{\mathrm{i}} \mathrm{a}_{\mathrm{i}} \qquad (4)$$

Barton et al. [37], in their phase equilibria studies, illustrated the diagram in Figure 5 for a wide range of sulfur activities and temperatures of sulfidation reactions.

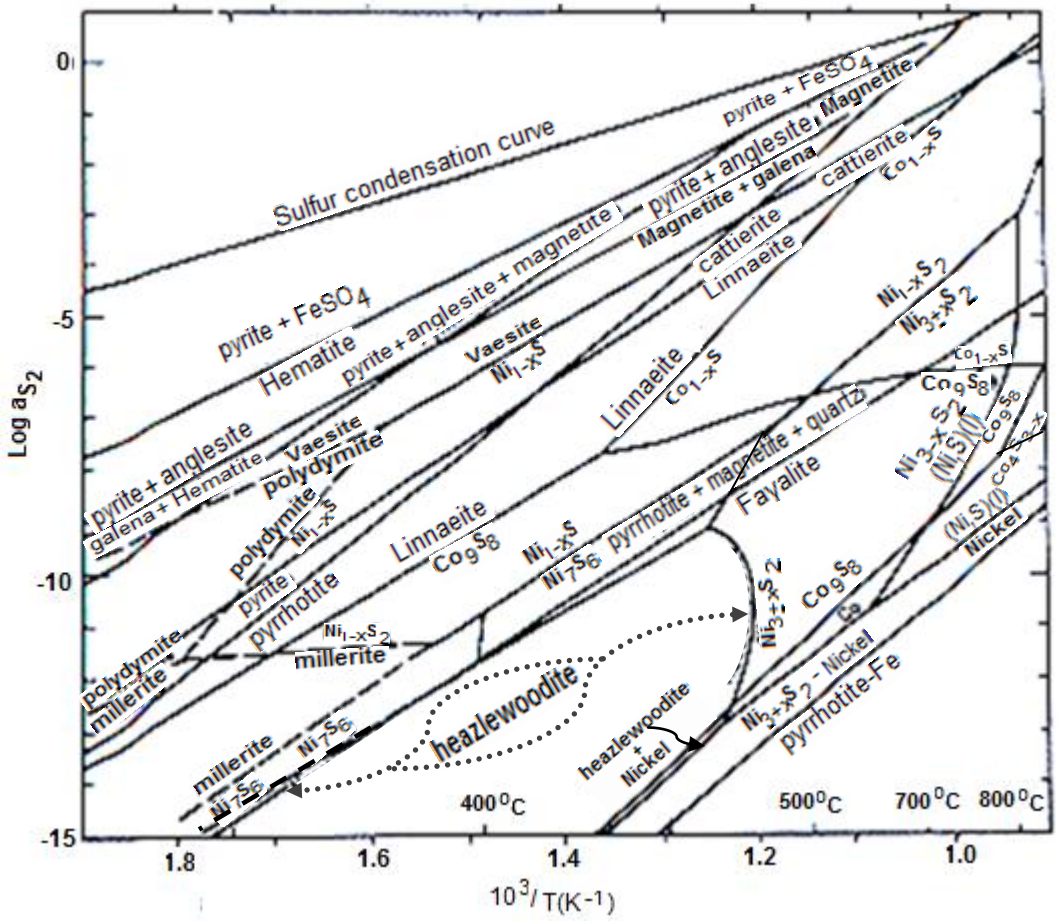

Figure 5. Activity of sulfur vs. inverse of temperature of some sulfidation reactions [37].

6.1 Sulfur Vapor and the Sulfur Liquid-Vapor Buffer

Sulfur vapor is a complex mixture of polymers of the type S_i (i = 1, 2 …8) whose relative proportions vary with the overall sulfur pressure and temperature. Most sulfidation reactions lie within the region where S_2(g), a widely used notion for sulfur species, exists. Braune et al. [38] introduced the standard data for relating total sulfur pressure to S_2 activity. According to Mills et al. [39], the total vapor pressure of sulfur can be given by the expression.

$$\log P(atm) = -6109.6411 \cdot T^{-1} + 16.64157 - 0.01705358 + 7.9769 \cdot 10^{-6} \cdot T^{2} \qquad (5)$$

Various methods of measuring sulfur activity are developed by different researchers. Their relative performances are summarized in Table 5. As indicated in Table 5, though with relatively lower speed of determination and inability to quench reactants the e.m.f method seems the best to measure $a_{S_2}(T)$. In the 1970s, the most widely used cell was Pt, Ag|AgI|$Ag_{2+x}S$, Pt, S_2(g). An electrochemical cells built by Schneeberg et al. [40] for sulfide research is shown in Figure 6 A, B and C below.

Table 5.Comparison of various methods for measuring S_2 activity as a function of temperature [4]. Notation: 3; excellent, 2; good, 1; fair, 0; poor, v; variable.

Feature compared	P_T	Dew point	e.m.f	Gas mixtures	Calori-metric	Gas mixture -tarnish	Electrum tarnish	Pyrrhotite indicator
Speed for individual	3	3	2	2	1	2	0	2
Speed for many determination	2	2	1	1	1	1	3	3
Ability to reach low temperature	1	2	3	1	3	2	3	3
S_2 range	1	2	3	2	3	2	2	2
Ability to quench	0	1	0	0	v	1	3	3
Precision	2	2	3	2	3	2	2	1
Ability to avoid thermal segregation	v	0	3	1	3	2	3	3
Tolerance for other	0	2	3	0	3	0	3	3
Ability to make many determinations on single preparation	3	3	3	2	3	2	0	0
Simplicity of apparatus	1	2	1	1	0	1	3	3

The voltage, e.m.f, of the cell (shown in Figure 6 (A)) is closely related to the fugacity of S_2(g) in equilibrium with argentite (at ~ 1 bar) through equation (6) [40]:

$$\ln f_{S_2} = [E - E^o(T)]\left({}^{4F}/_{RT}\right) + \ln f^o_{S_2}(T) \qquad (6)$$

where E is the measured e.m.f, E^o is e.m.f of the cell at the fugacity ($f^o_{S_2}$) of the sulfur condensation curve at a given T, and F is Faraday's constant. The operational limits of the electrochemical cell were roughly between 150 - 450^{o}C, as illustrated in Figure 7. The low temperature limit was dictated by the acanthite-argentite transition in Ag_2S and the high limit by the onset of significant electronic conduction in the AgI electrolyte.

Another cell described by Sato et al. [41] utilized Ag-saturated beta-alumina as an electrolyte and can be operated to considerably higher temperature. It has been used to measure sulfur activities in natural processes. Kissin et al. [31] described a novel application in which the Ag|AgI|$Ag_{2+x}S$ cell is used on a precession X-ray camera to measure sulfur activity of a heated crystal while X-ray photographs are being taken.

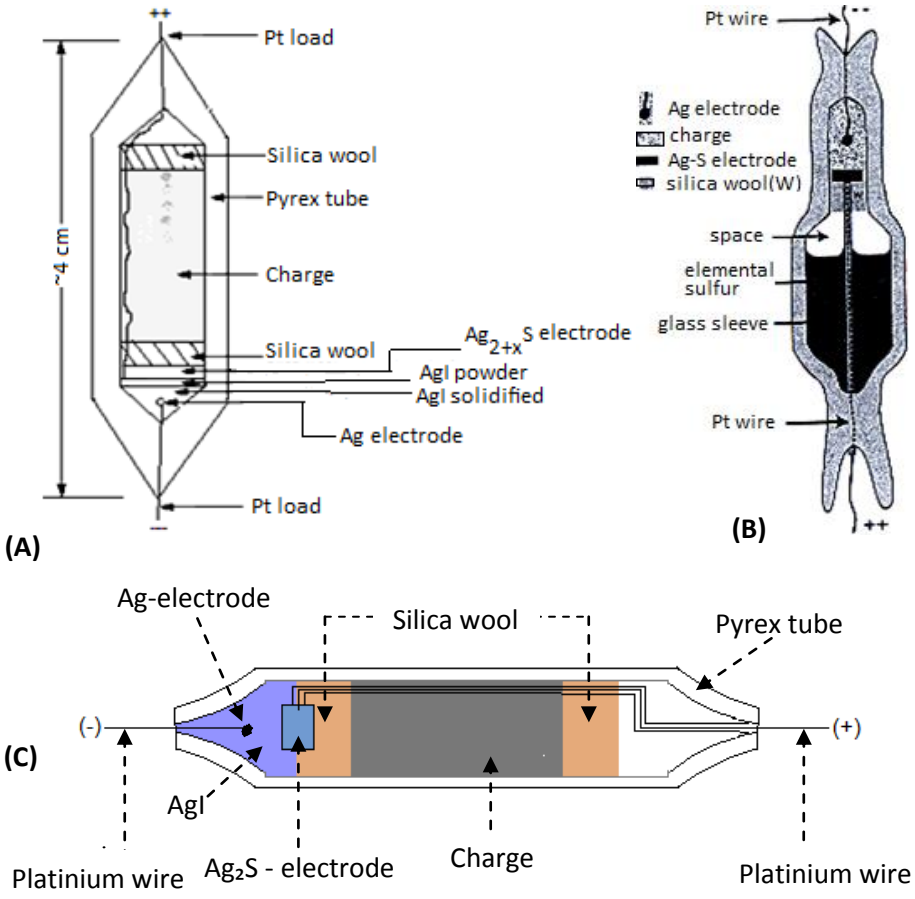

Figure 6. (A) & (C) typical Ag|AgI|$Ag_{2+x}S$ cell used to measure f_{S_2} buffered by a mineral assemblage, (B) Cell used for E^{o} calibration [40].

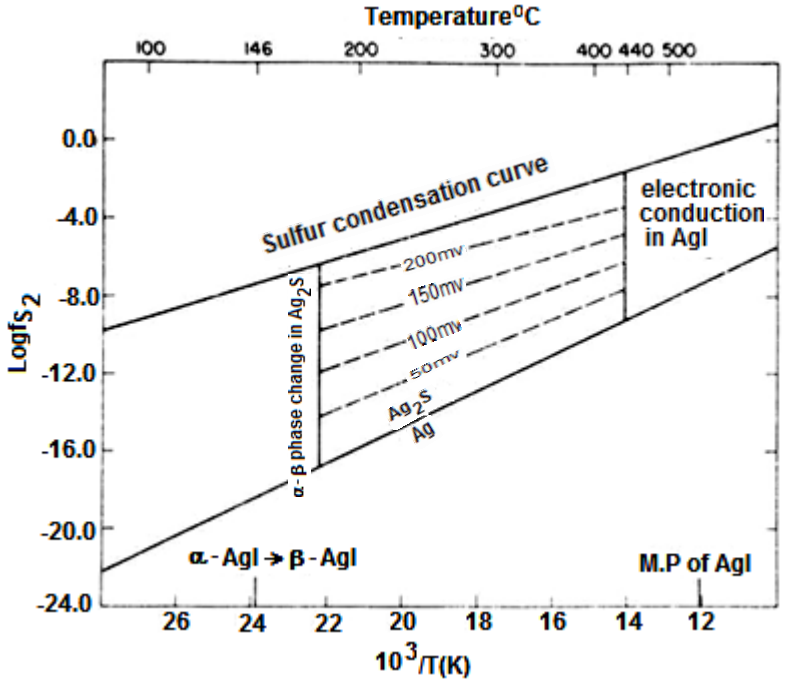

Figure 7. Operational limits of the Ag|AgI|$Ag_{2+x}S$ cell. Dashed lines show the e.m.f responses [40].

7 Sulfide Phase Equilibria

Present knowledge of sulfide phase equilibria is the result of both laboratory experiments and the conclusions drawn from natural sulfide minerals. The study of phase equilibria involves the determination of the physical relations among either natural or synthetic materials. The objective of such studies is to determine the existence of phases at equilibrium and the interdependence of composition, thermal and pressure stabilities, and activities of phases.

These studies have contributed to the understanding of; processes involved in the beneficiation of minerals and refining, the distribution of elements between minerals and the conditions under which various sulfide phases may exist. In this section, the techniques employed in the determination of the sulfide phase equilibria along with methods of illustrating them are discussed. Examples from several important binary and ternary sulfide systems are included.

7.1 Binary Sulfide Systems

Experimental studies to determine the presence or absence of equilibrium is complex. In reality it is often not possible to unequivocally prove equilibrium; however, there are tests which are commonly applied, such as:

(I) Persistence of an assemblage unchanged through time under a static set of conditions

(II) Reversibility of a reaction, i.e., definition of some boundary which when crossed causes change in an assemblage, but when re-crossed to the initial conditions results in reestablishment of the initial assemblage

(III) Synthesis of the same assemblage from different sets of reactions, e.i., $Fe + S_{(liq)} \rightarrow FeS$ or $Fe + FeS_2 \rightarrow 2FeS$.

Hence, the evidence for equilibrium in minerals is often taken to be the absence of evidence for disequilibrium, that is, zoned crystals. Fortunately, for the sulfide mineralogist, synthetic phase equilibria studies frequently have passed the tests for equilibrium and have yielded data sufficiently similar to natural occurrences to provide some assurance of their reliability. Survey of data by different investigators on some sulfides stability, as summarized by Craig et al. [42], is listed in Table 6.

Table 6. Summary of studies by different investigators on the maximum thermal stabilities of (Fe, Cu, Ni, Zn)-S systems [42].

System	Compound	Mineral name	Maximum thermal stability(°C)
Fe-S	FeS	troilite	140
	FeS_{1-x}	mackinawite	?
	$Fe_{1-x}S$	hexagonal pyrrhotite	1190 (Stable only above ~100)
	$Fe_{1-x}S$	MC pyrrhotite	308
	$Fe_{1-x}S$	NA pyrrhotite	266
	$Fe_{1-x}S$	NC pyrrhotite	213
	Fe_9S_{10}	5C pyrrhotite	~100
	$Fe_{10}S_{11}$	11C pyrrhotite	~100
	$Fe_{11}S_{12}$	6C pyrrhotite	~100
	$Fe_{7\pm x}S_8$	monoclinic pyrrhotite	254
	$Fe_{7+x}S_8$	anomalous pyrrhotite	?
	Fe_2S_3	γ-iron sulfide	?
	Fe_9S_{11}	smythite	~ 75
	Fe_3S_4	greigite	--
	FeS_2	pyrite	572
	FeS_2	marcasite	--
Cu-S	Cu_2S	Chalcocite	103
	Cu_2S	-	~435
	Cu_2S-Cu_9S_5	-	1129
	Cu_2S	-	>500
	$Cu_{1.97}S$	djurleite	93
	Cu_9S_5	digenite	83
	Cu_7S_5	anilite	70
	$Cu_{1+x}S$	blue-remaining covllite	157
	CuS	Covellite	507
	CuS_2	-	>550
Ni-S	Ni_3S_2	heazlewoodite	556
	$Ni_{3\pm x}S_2$	-	806
	α-Ni_7S_6	godlevskite	400
	Ni_7S_6	-	573
	NiS	millerite	379
	α-$Ni_{1-x}S$	-	992
	Ni_3S_4	polydymite	356
	NiS_2	Vaesite	1007
Zn-S	ZnS	sphalerite	-
	ZnS	wurtzite	-

7.1.1 Fe-S System

Besides containing two of the most common sulfide minerals, pyrite and pyrrhotite, the Fe-S system is a cornerstone to the understanding of phase relations and thermochemistry of many other important systems including Zn-Fe-S, Cu-Fe-S, Ni-Fe-S and Fe-As-S. The basic phase diagram above 400°C is shown in Figure 8.

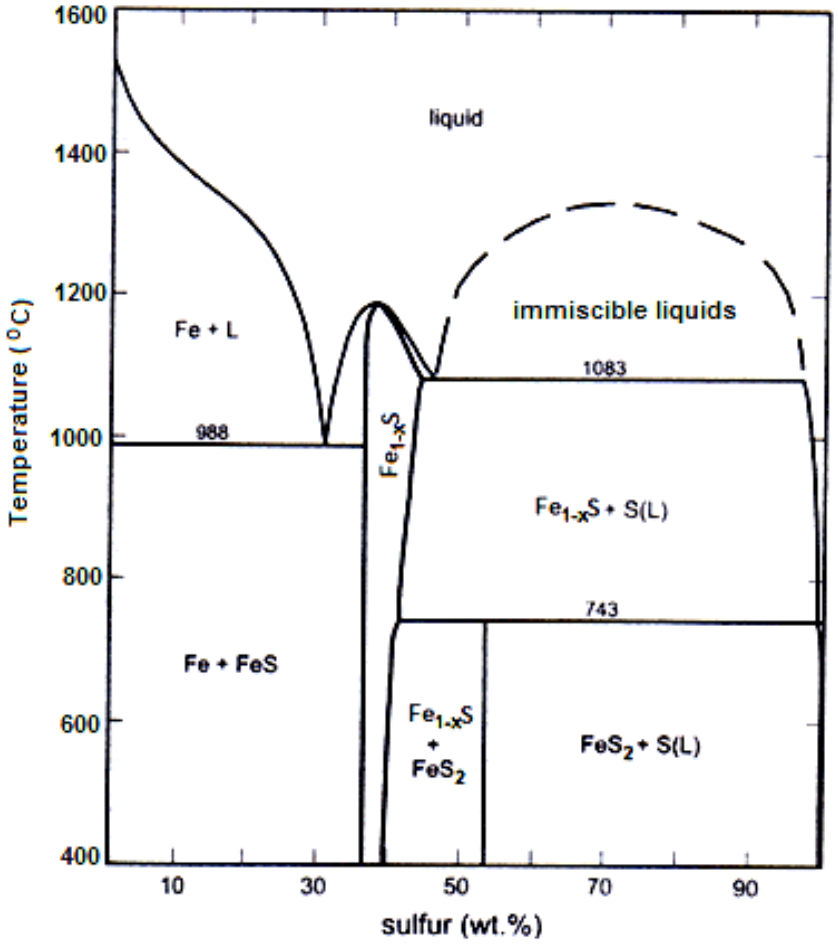

Figure 8. Relations among condensed phases in the Fe-S system above 400°C [43].

7.1.1.1 Troilite (FeS), Mackinawite (FeS_{1-x}) and "Hexagonal" Pyrrhotite ($Fe_{1-x}S$)

Strictly speaking, the name troilite applies only to the polymorph of stoichiometric FeS which is stable below 140°C [44, 45]. Above 140°C, FeS has the NiAs (1C) (Appendix A) structure of high-temperature hexagonal pyrrhotite whose composition range extends for a considerable distance across the system. It usually appears as low-temperature hexagonal pyrrhotite. The solvus separating troilite from other pyrrhotites has been determined by Yund et al. [45].

Mackinawite invariably contains some Co and Ni though these elements are not essential as demonstrated by Berner et al. [46], who precipitated the phase from aqueous iron sulfide solutions between 20° and 95°C. The metal to sulfur ratio in mackinawite is slightly greater than unity (1.04 to 1.07; [47]) and the formula is usually written as $Fe_{1+x}S$. However, there is a deficiency of sulfur in the structure rather than an excess of metal so the formula is properly written as FeS_{1-x} [23].

Until the year 1973 very little was known about the thermal stability of mackinawite, as a result it was not included in phase diagrams as a stable phase. Zoka et al. [48] found that natural mackinawite from a variety of localities breakdown non-isochemically between 120°C and 153°C to pyrrhotite of a more S-rich composition. However, they concluded that their experiments did not

represent equilibrium because the expected breakdown of the assemblage of metallic Fe, Co, Ni + troilite was not found.

Pyrrhotite has been relatively studied well than any other sulfide mineral; however, many enigmas remain, particularly at low temperatures where slow reaction kinetics tends to obscure the phase relations. Nonetheless, studies at low temperatures by Nakazawa et al. [49] and Kissin et al. [31], in which single crystal X-ray diffraction was used as an analytical tool, have reduced what before was chaos to mere confusion.

Between 1190°C (T_m) and 308°C, the full width of the pyrrhotite phase field is occupied by a single solid solution, $Fe_{1-x}S$, in which iron and vacancies are randomly distributed in the cation sites of the NiAs (1C) structure. This phase also extends to lower temperatures but with a more restricted composition range. Neel transition does not accompany a phase change [31, 49, 50]. Superstructures formed may correlate with some lower temperature phases are formed during quenching [51].

7.1.1.2 Monoclinic Pyrrhotite ("Fe_7S_8")

Ferromagnetic pyrrhotite with a monoclinic superlattice and composition centered about Fe_7S_8 has been known as a mineral for decades [52] and synthesized repeatedly in an evacuated silica tubes. However, earlier experimental studies by Clark et al. [53], Arnold et al. [54], Yund et al. [55] and Taylor et al. [30], to name just a few, gave results that were conflicting and were plagued by demonstrable, extensive metastability. Such metastability in an evacuated silica tube experiments was not surprised Yund et al. [56] because they observed that pyrrhotite oversaturated with respect to pyrite (by as much as 0.18 at. % Fe) did not nucleate pyrite after annealing (at 325°C) for more than a year. More recently Kissin et al. [31] and Rising et al. [57] have used the method of hydrothermal recrystallization to overcome these kinetic difficulties and established phase relations for monoclinic pyrrhotite which are internally consistent and devoid of obvious metastabilities. Kissin et al. [31] has synthesized single crystals of monoclinic pyrrhotite in the temperature range of 115 -254°C and obtained a close control on the compositional limits of this mineral. Monoclinic pyrrhotite has variable stoichiometry. It is only nominally Fe_7S_8 and is separated from the NA and NC-type pyrrhotites by narrow solvi. Kissin's et al. [31] upper stability limit of 254°C for monoclinic pyrrhotite going to NA pyrrhotite + pyrite has been reversed. It was in good agreement with the indirect determination at 251 ± 3°C by Rising et al. [57], but considerably lower than previous estimates in the range 292° - 325°C, using the aforementioned evacuated silica tube experiments.

7.1.1.3 Gamma Iron Sulfide (Fe_2S_3) and Smythite (Fe_9S_{11})

Gamma Iron Sulfide (Fe_2S_3) phase has not been encountered in nature but has been precipitated from an aqueous sulfide solution at 60°C by Yamaguchi et al. [58]. Electron diffraction patterns indicate that it has a spinel structure similar to greigite (Fe_3S_4), the main difference in their patterns being the intensities of some of the reflections. Like greigite it is magnetic, and Yamaguchi et al. [58] suggested that γ-Fe_2S_3 bears the same relation to greigite as γ-Fe_2O_3 (maghemite) does to magnetite (Fe_3O_4).

Smythite was originally described by Erd et al. [59] as having a rhombohedral structure and a Fe_3S_4 composition which led Kullerud et al. [60] to believe that it was a polymorph of greigite. However, after an extensive re-examination of naturally occurring smythites, Taylor et al. [61] have redefined the mineral as having a pseudorhombohedral structure related to that of monoclinic pyrrhotite and a composition $(Fe,Ni)_9S_{11}$ (~$(Fe,Ni)_{3.25}S_4$). This composition was also found by Nickel et al. [62] and Bennett et al. [63]. Thus, smythite ($(Fe,Ni)_9S_{11}$) is not a polymorph of greigite but may be another ordered pyrrhotite of the $Fe_{n-1}S_n$ clan. It occurs as exsolution lamellae in monoclinic pyrrhotite [63] and in geodes which have fluid inclusion filling-temperatures of 25 to 40°C, suggesting that it is a phase stable only at low temperatures. However, the stability of smythite was not well known. Kissin et al. [31] did not encounter smythite in his hydrothermal recrystallization experiments above 115°C. Smythite has been precipitated from aqueous sulfide solutions [64]. Taylor et al. [30] found that smythite began to break down at 210°C in nonequilibrium experiments but concluded that it must be stable below 75° because he was unable to synthesize it at higher temperatures. The fact that all natural smythites contain 0.4 to 7.5 wt. % Ni suggested to Taylor et al. [61] that it might be a phase in the ternary Fe-Ni-S system.

7.1.1.4 Pyrite and Marcasite (FeS_2)

Pyrite is stable up to 743^{o}C beyond which it undergoes a peritectic breakdown to hexagonal 1C pyrrhotite + sulfur. The relationship between pyrite and its polymorph marcasite was intensively studied by many researchers, during the years 1934-1974. Despite that the relationship remained unclear. In 1934 a scientist concluded, on the basis of selected superior chemical analysis, that the minerals are slightly different in chemical composition; marcasite was found to be slightly sulfur deficient (i.e. FeS_{2-x}) relative to the pyrite which was assumed to be nearly stoichiometric FeS_2. This idea has been disproved by other researchers in 1959, claiming that the precision of sulfur analyses did not warrant it. Nevertheless, electrical measurements by two different researchers, in 1968, demonstrated a measurable nonstoichiometry in pyrite. Furthermore, marcasite could be inverted to pyrite as low as 150^{o}C in the presence of excess sulfur [60]; this suggested to them that sulfur in excess of the Fe:S ratio in marcasite is a necessary constituent of pyrite. They also described experiments which showed that coexisting marcasite + pyrite could be synthesized up to 432^{o}C (at 2kb) in the presence of water but not in its absence. As a result it has been calculated that H-S bonds might stabilize marcasite although an alternative explanation of the experiment was that the activity of sulfur was buffered within a range where marcasite is stable. Because of the inversion rate of marcasite to pyrite above 157^{o}C is directly proportional to temperature and inversely proportional to grain size, Rising et al. [57] concluded that marcasite is metastable relative to pyrite and pyrrhotite ($Fe_{(1-x)}S$ (x = 0…0.2)) in the temperature range. This was later supported by Kissin et al. [31] as they didn't encounter marcasite while conducting an experiment at about 115^{o}C.

The marcasite/pyrite polymorph pair is probably the most famous polymorph pair next to the diamond/graphite pair. The mineral marcasite, sometimes called white iron pyrite, is lighter and more brittle than that of the pyrite. Specimens of marcasite often crumble and break up due to the unstable crystal structure.

7.1.2 Cu-S System

Chalcocite and covellite were the two first ever known sulfide minerals in the Cu-S system. After 1942 more sulfide minerals and phases were revealed as listed in Table 7. After Roseboom's et al. [65] study on degenite, as described in Table 7, Morimoto et al. [66] reported that digenite to be stable only when it contains a small amount of iron (~1%) and redesigned it as the Cu-Fe-S system. Above 500°C the phase relationships are straight forward (See Figure 9); two intermediate phases, cubic solid solution series which ranges in composition from chalcocite to degenite and covellite, which is stable at the presence of its autogenous vapor pressure up to 507°C. Thermochemical aspects of the Cu-S system have been summarized by Barton et al. [67], as shown in Figure 10.

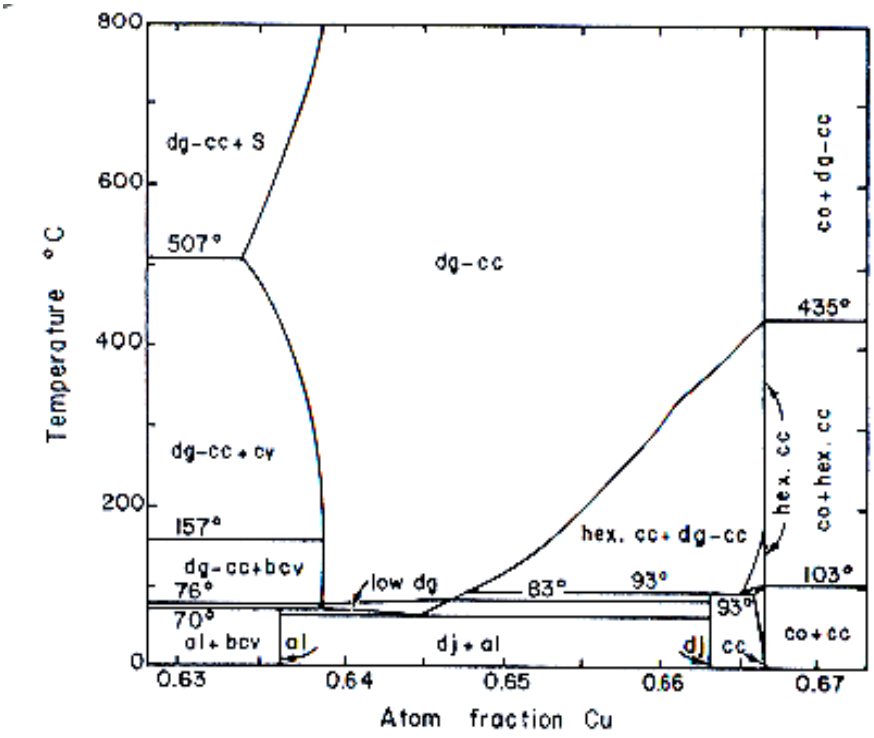

Figure 9. Phase relations in a portion of the Cu-S system [67].

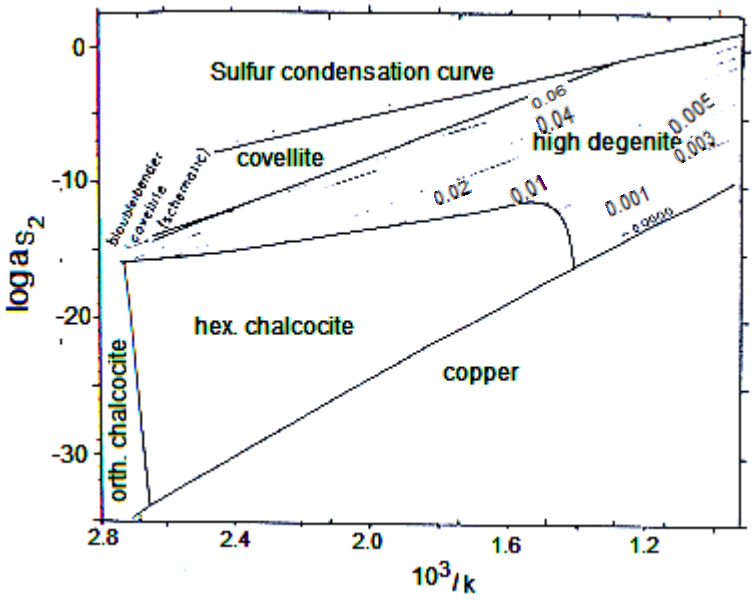

Figure 10. Diagram of activity of sulfur vs. inverse of temperature for the Cu-S system [67]. The composition of high degenite is shown in light weight contours: the numbers indicate the ratio S_2/Cu_2S in the solid solution.

Schneeberg et al. [40] has measured the fugacity of S_2 (g) over the covellite - high digenite assemblage ($2Cu_2S$ (in cc-dg) + S_2 = 4CuS) by means of electrochemical cells. Their two equations determined in separate experiments are expressed as equations (7) and (8).

$$\log f_{S_2} = 24.467 - \frac{25669}{T} + \frac{4844700}{T^2} \quad (7)$$

$$\log f_{S_2} = 24.193 - \frac{24097}{T} + \frac{4211000}{T^2} \quad (8)$$

7.1.2.1 Crystal Chemistry and phases in the Cu-S System

Copper in sulfides may assume either a tetrahedral or triangular coordination. Copper and silver sulfides exceptionally frequently display rapid phase transformation at very low temperatures. At 104°C chalcocite transforms rapidly to a hexagonal form whose unit cell corresponds to that of an hcp S array. The electrical conductivity and the diffusion coefficient for Cu in this phase are quite large. At about 350°C a further phase transformation takes place to a cubic phase of broad stoichiometry known as digenite [68]. Anilite (Cu_7S_4) is orthorhombic (pseudo cubic) and transforms readily up on grinding to a metastable form of digenite. A small deficiency of Cu in chalcocite results in a new phase called djurleite ($Cu_{1.96}S$), which would appear to have a structure closely related to that of chalcocite.

Chalcocite (Cu_2S), reported by Evans et al. [69] to be monoclinic, is stable only up to 103°C, above which it inverts to a hexagonal form (stable up to ~435°C). Tetragonal Cu_2S is only stable at pressures above ~0.8Kb, as shown in Figure 11. Although the tetragonal form of Cu_2S can be readily quenched in the laboratory, Skinner et al. [70] reported that it inverts to chalcocite when stored at

room temperature for a few weeks. However, Serebryanaya et al. [71] reported no change in his synthetic tetrahedral Cu_2S after 8 months.

Table 7. Minerals and phases of the Cu-S system [42].

Mineral name	Composition	Thermal stability(°C)		Remarks
		Max.	Min.	
Chalcocite	Cu_2S	103	-	Inverts to hexagonal form
-	Cu_2S	~435	103	Inverts to cubic form
-	Cu_2S	1129	~435	Complete s.s. with Cu_9S_5
-	Cu_2S	500	-	Stable only at P>1Kb
Djurlite	$Cu_{1.97}S$	93	-	-
Digenite	Cu_9S_5	83	-	Stabilized by Fe
-	$Cu_{9+x}S_5$	1129	83	Complete s.s.
Anilite	Cu_7S_5	70	-	Complete s.s. with Cu_2S
"Blaubleibender"Covellite	$Cu_{1+x}S$	157	-	Thermodynamically stable?
Covellite	CuS	507	-	-
-	CuS_5	550	-	High- P synthesis. Pseudo cubic?

The low temperature cubic form of digenite becomes a stable phase on the Cu-S joint, above ~70°C. At slightly higher temperature (76 - 83°C), based on the composition, degenite inverts to a high temperature cubic form which is isostructural with high temperature chalcocite. Up on further heating djurleite ($Cu_{1.97}S$) with maximum thermal stability of 93°C (Table 7), decomposes to the hexagonal form of chalcocite and the cubic cc-cg phase. Anilite (Cu_7S_5), above its maximum thermal stability (~70°C) decomposes to degenite and covellite [66]. Anilite, like djurleite, closely resembles digenite and is difficult to recognize without careful X-ray examination.

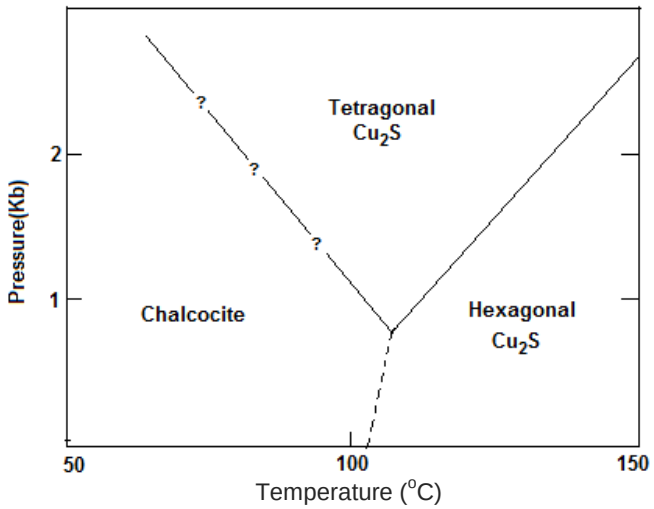

Figure 11. Schematic representation of the Cu_2S phase diagram [70].

7.1.3 Ni-S System

The mineralogy and phase equilibria of the binary Ni-S system seem to be relatively well understood. A summary of minerals and phases in the Ni-S system is given in Table 8. The phase equilibria diagram is shown in Figure 12.

Table 8. Minerals and Phases in the Ni-S system [42].

Composition	Mineral name	Thermal stability (°C)		Structure type (cell edges in Å)	Remarks
		Maximum	minimum		
Ni_3S_2	Heazlewoodite	556	-	Hexagonal R32	
$Ni_{3+x}S_2$	-	806	524		lower
α-Ni_7S_6	Godlevskite	400	-	Orthorhombic	
Ni_7S_6	-	573	400		
NiS	Millerite	379	-	Hexagonal R3m	
α-$Ni_{1-x}S$	-	999	282	Hexagonal	Lower
Ni_3S_4	Polydymite	356	-	Cubic Fd3m	
Ni_8S_2	Vaesite	1007	-	Cubic Pa3	

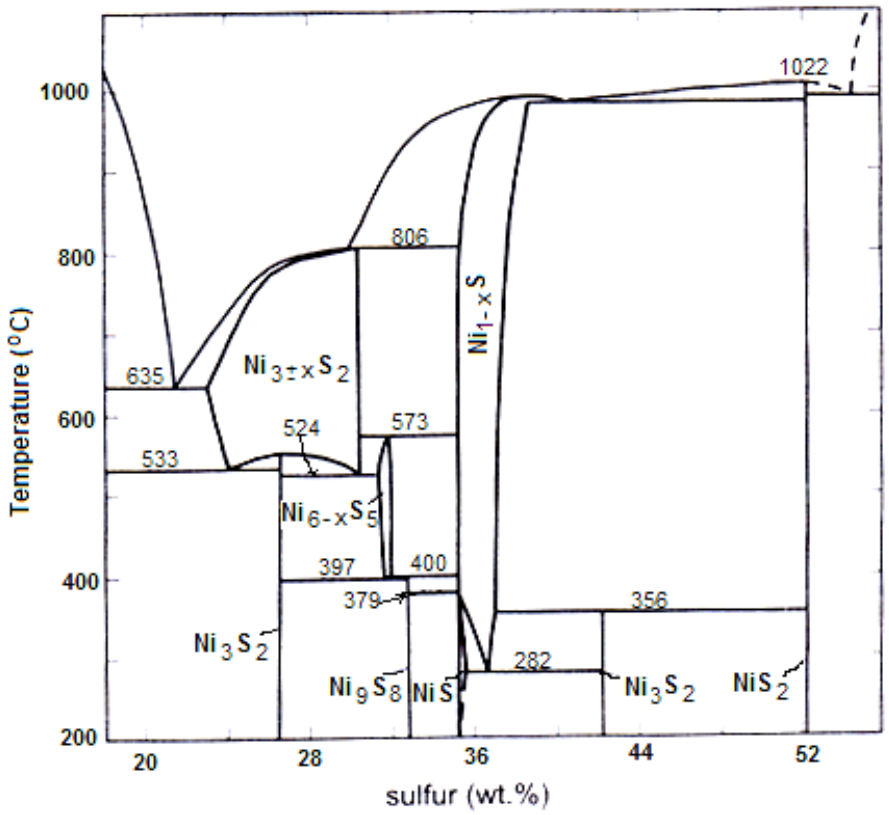

Figure 12. Phase relations in the Ni-S system in the composition range of 18-56 wt. %S, at the presence of an equilibrium vapor pressure [72].

In contrast to the Fe-S and Cu-S system the Ni-S system appears to have no phases with low thermal stabilities or multiple structures. Phase equilibria studies revealed phases with relatively

high breakdown temperatures, rapid and reversible transitions, and relatively uncomplicated structures.

7.1.4 Zn-S System

Sphalerite (ZnS) and wurtzite (ZnS) are commonly regarded as the low-temperature cubic and high-temperature hexagonal polymers, respectively. At about 1 atm, the transition from the sphalerite form to the wurtzite form occurs at about 1020 ^{o}C. Wurtzite which is naturally formed at very lower temperatures was generally thought to be metastable. However, in the early 1970s this was proved to be not the case. Zinc sulfide is known to be nonstochiometeric and, although the composition range is small, it was shown by Scott et al. [73] to have an unusually large effect on the temperature of the polymorphic transition between the sphalerite and wurtzite. In 1974 a researcher suggested the temperature of the inversion to be 1031^{o}C for S-rich and 1013^{o}C for Zn-rich zinc sulfides. Sphalerite at about 900^{o}C may exist in equilibrium with sulfur and zinc.

Scott et al. [73] maintained that wurtzite is sulfur-deficient relative to the sphalerite and both minerals have a combined non-stoichiometry on the order of 0.9 atomic percent. A similar conclusion was reached by some other scientists (1965), who reported that sphalerite inverted to the wurtzite at the presence of zinc vapor, and wurtzite inverted to the sphalerite under a sulfur pressure.

7.2 Ternary Sulfide Systems

In this section the works of Scott et al. [74], Barton et al. [75] and Manning et al. [76] on the Fe-Zn-S system; Cabri et al. [77] on the Fe-Cu-S system; and Kullerud et al. [78], Rajamani et al. [22], Bell et al. [79] and Vaasjoki et al. [80] on the Fe-Ni-S system related to the most important ores in the base metals smelting such as, pentlandite ((Ni, Fe)$_9$S$_8$), chalcopyrite (CuFeS$_2$) and sphalerite (Zn, Fe)S are summarized.

7.2.1 Fe-Zn-S System

This system involves additional phases like sphalerite and wurtzite than discussed in the Fe-S system. Sphalerite has a cubic close packed structure (F43m) in which every other tetrahedral site is occupied by Zn (illustrated in Appendix A). Using infrared absorption spectra results, Manning et al. [76] claimed that as much as 10% of the Fe in sphalerite is octahedral Fe^{3+}. Although this was later disproved by other investigators by indicating that all of the irons are tetrahedral Fe^{2+} [81].

The compositions of coexisting sphalerite and pyrrhotite solid solutions in the Fe-Zn-S system have been investigated in the temperature range 580 - 850^{o}C at low pressure by Barton et al. [75]. These investigators, as well as Scott et al. [74, 82], have estimated the activity coefficient of FeS in sphalerite (γ_{FeS}^{sp}) from the relationship between the activity of FeS in pyrrhotite (a_{FeS}^{po}) and mole percent of FeS in sphalerite. This is equivalent to considering (Zn, Fe)S as a solution of sphalerite (ZnS) and troilite (FeS). However, the mixing behavior of ZnS and FeS in sphalerite can be determined more conveniently from data referred to the metastable FeS end-member, isostructural with sphalerite.

Generally, the system was studied under the pseudo phase diagram of FeS-ZnS-S system (Appendix B), where activity of FeS varies at different fugacity of sulfur and temperature as well as its concentration in sphalerite. In studying the effect of pressure on the sphalerite + pyrite + pyrrhotite solvus, Scott et al. [82] presented the T-X projection of the phases isobars as shown in Figure 13. The 7.5kb considerable curvature, as shown in Figure 13, suggest that there may be a large variation with temperature in a_{FeS} at high pressure.

Other elements in the Fe-Zn-S system are likely to have much effect on the phase relations in the T-X diagram illustrated in Figure 13. Only rarely will Co and Ni be in high enough concentration, in the iron sulfides, to cause a significant decrease in a_{FeS} [75]. Of the remaining elements commonly found in sphalerite, only Cu is problematic. The Cu content of most of sphalerites is usually less than 1 or 2 wt. %, but the common occurrence of chalcopyrite exsolution blebs indicates that solid solution was much greater at high P and T. There were very few data on phase relations in the Cu-Fe-Zn-S system (1974), but there were indications for the $CuFeS_2$-ZnS join to be truly binary, i.e., there is a substitute like CuFe = 2Zn.

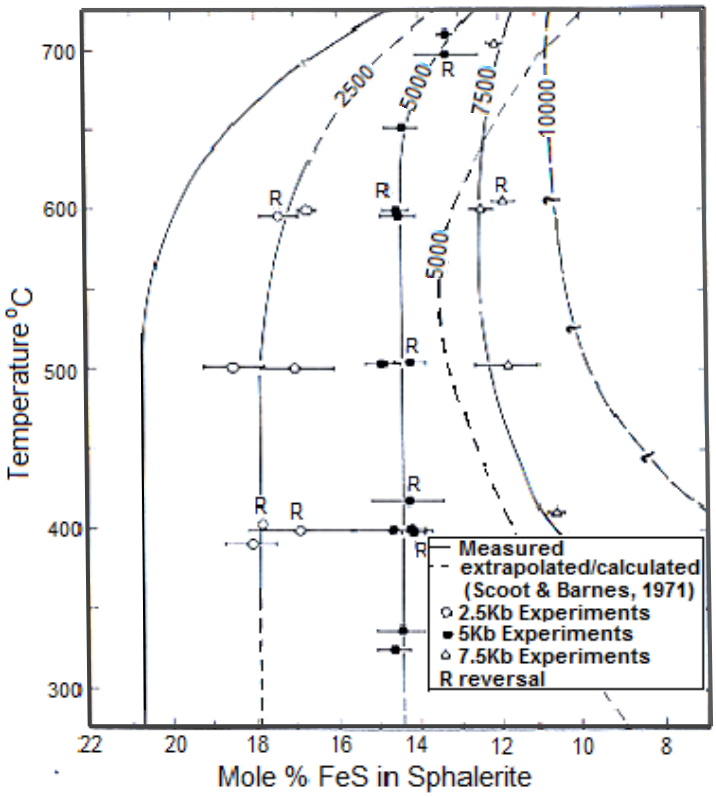

Figure 13. T-X projection of the sphalerite + pyrite + hexagonal pyrrhotite solvus isobars [82].

7.2.2 Fe-Cu-S System

The Cu-Fe sulfides phase equilibria and mineralogical relations are relatively extensively studied. In spite of this many relationships in the system remained enigmatic, obscured by the presence of

extensive solid solutions, unquenchable phases, and metastability. As that of the phases in the Cu-S system, the maximum stability range was determined to be 1129°C, which for ~$(Cu, Fe)_9S_5$.

The nature of the high temperature relationships in this system is well established after Cabri et al. [77] studied a 600°C isothermal condition and illustrated it as a ternary phase diagram, of which section is shown in Figure 14. However, a lot remained to be learned about the phase equilibria of the system, especially below 400°C.

The centrally located sphalerite-type (fcc) structure includes a large compositional area which is slightly sulfur deficient. Cabri et al. [77] has noted that the iss field may be divided into three zones each characterized by different quenching behavior. Compositions in the first zone, which includes the S-rich portion of the iss from Cu:Fe=1 to the Fe-rich extremity, quench from 600°C to give chalcopyrite + iss. The second zone, which includes the S-deficient region on the Fe-rich end, quenches to a phase exhibiting a primitive cubic cell. The third zone which separates zone 1 and 2 and which includes all of the central and Cu-rich portions of the iss quenches to give the primitive phase plus either chalcopyrite ($CuFeS_2$) or mooihoekite ($Cu_9Fe_9S_{16}$).

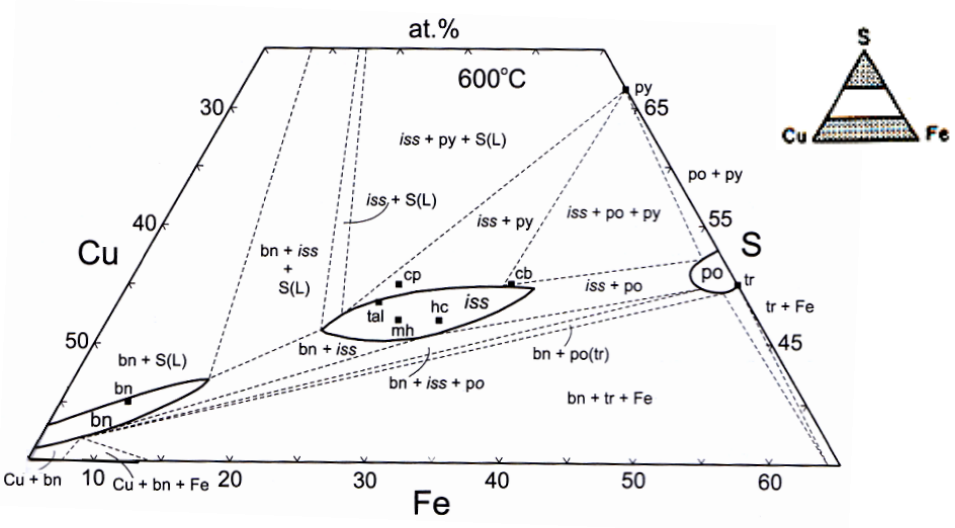

Figure 14.Phase relations in the central portion of the Cu-Fe-S system at 600°C [77].

As temperature decreases below 600°C the simple well understood phase equilibria gradually give way to a less understood and, in some areas, quite conjectural relationships as additional phases become stable. The most important change was the appearance of chalcopyrite as a stable phase below 557°C. It forms in the iss-pyrite field and remains isolated from all other Cu-Fe sulfides until temperature is further decreased. Other noted phases as a consequence were covellite at 507°C and idaite ($Cu_{5+x}FeS_{6+x}$) at 501°C.

7.2.2.1 iss and pc

At temperatures above 500°C the iss represent the dominant ternary phase of the Cu-Fe-S system. Long believed to be a high temperature polymorph of chalcopyrite, the iss was later known to represent a distinct phase. There is, however, a close relationship between the disordered cubic

structure of the iss (a ≈ 5.36Å) and the ordered tetragonal cell of the chalcopyrite (a = 5.28Å; c = 10.40Å). Composition of the iss varies over a wide range (see Figure 14). Much of the misinterpretations in the past might have resulted from the nonquenchability of the large portions of the compositional range.

The low-temperature decomposition of the iss was not well understood but it appeared that zone 2 in Figure 14 inverts at some temperature below 600°C to pc which persists down to the range of 20 - 200°C. Natural intergrowths of chalcopyrite and bornite, chalcopyrite and cubanite, mooihoekite and haycockite, and natural assemblages of talnakhite ($Cu_9(Fe, Ni)_8S_{16}$) most likely formed as decomposition products of initially deposited iss.

7.2.3 Fe-Ni-S System

The high temperature equilibrium of the Fe-Ni-S system is dominated by the $(Fe,Ni)_{1-x}S$ solid solution (mss) which spans the system from a temperature of nearly 1000°C to below 300°C. Decrease in temperature from 1000 °C results in the appearance of several binary phases and the development of a variety of 2- and 3- phase regions as shown in Figure 15 and Figure 16.

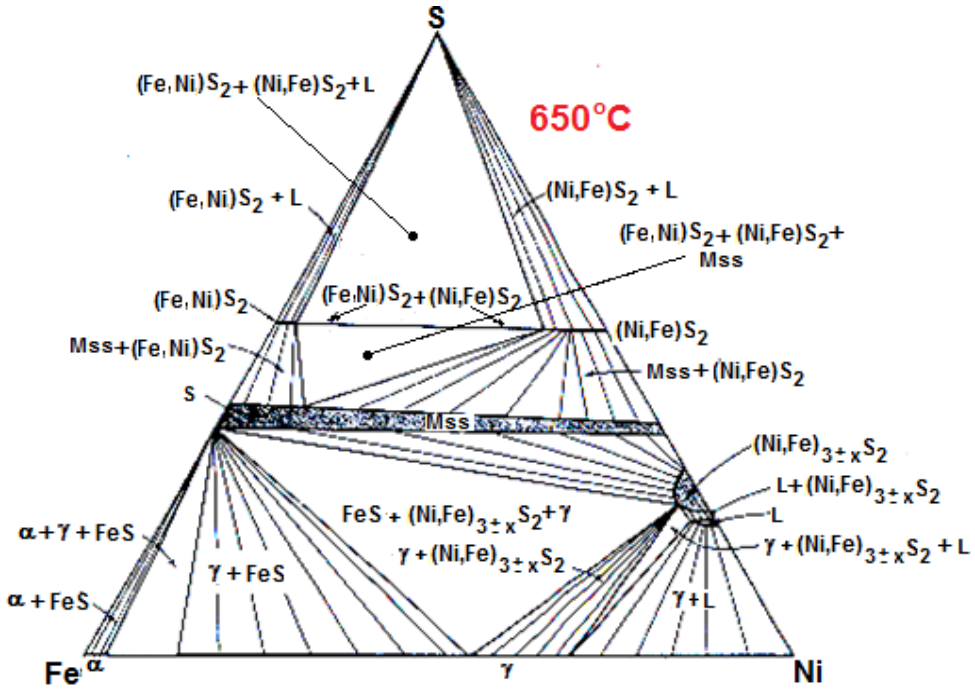

Figure 15. Phase relation in the Fe-Ni-S system at 650°C in the presence of an equilibrium vapor [83].

In this temperature range, relatively little change was noted in the compositional limits of the mss. Pentlandite ($(Fe,Ni)_9S_8$), the principal ore mineral of nickel, stabilizes at 610 °C [78], forming through a reaction of a nearly pure FeS composition of the mss and $(Fe,Ni)_{3\pm x}S_2$.

Natural pentlandites frequently contain small amounts of Co substituting for Fe and Ni. Vaasjoki et al. [80] have shown that the presence of Co to raise the thermal stability of the pentlandite (in pure Fe-Ni-S system stable up to 610 °C). For example, the maximum thermal stability of a specimen with 7.5 wt. % Co is 630°C and that of a specimen with 40.8 wt. % Co is 746°C. Pentlandite structure, cubic (Fm3m), is based on a "cube cluster" of tetrahedral cations [22].

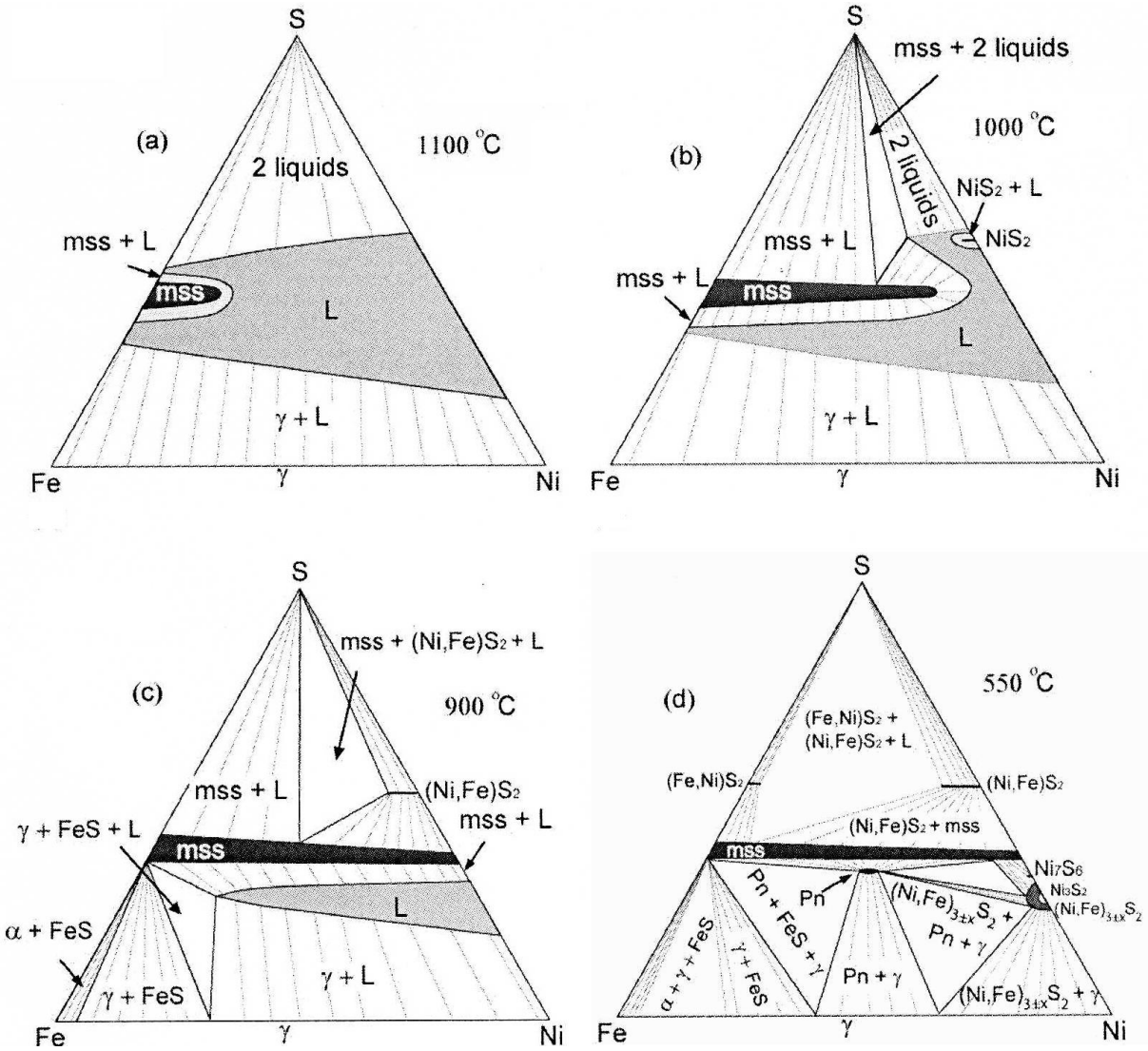

Figure 16. Phase relations in the Fe-Ni-S system at (a) 1100°C (b) 1000°C (c) 900°C (d) 550°C (after Kullerud and Yund, 1969); for the purpose of clear illustration, some parts of the diagrams are enlarged [84].

The open nature of the pentlandite structure is responsible for two interesting phenomena. Bell et al. [79] found that confining pressure reduces the thermal stability of pentlandite to 425°C at 25Kb, and Morimoto et al. [85] reconfirmed that pentlandite has an unusually large coefficient of thermal expansion. Violarite ($FeNi_2S_4$) is a thiospinel and occurs commonly as an alteration product of pentlandite. It forms a complete solid solution with polydymite (Ni_3S_4) at temperatures below 360°C. Increase in pressure reduces the maximum thermal stability of the violarite-polydymite

series (Wiggins and Craig, unpublished). Equilibrium relationships within the Fe-Ni-S system below 200°C are ambiguously established and have been frequently confused by disequilibrium.

7.3 Sulfosalts

Sulfosalts are similar to most silicates in that they are commonly intermediate phases along the joining line between simple compounds. Most sulfosalts can be regarded as intermediate phases on joins between simple sulfides [86, 87].

The term sulfosalts have been sources of confusion for decades. Hellner et al. [88], Nowacki et al. [89] and Takeuchi et al. [90] have defined in terms of structural units, i.e, the presence of the TS_3 (T=As, Bi and Sb) pyramids in the structure distinguishes a sulfosalt from a sulfide. Sulfosalts may be represented by a simple general formula: $M_xT_yS_z$.

Many sulfosalts lie along the metal-sulfide – semi metal-sulfide joins and may be characterized by relatively simple stoichiometries. For example, Skinner et al. [91] found chalcostibite ($CuSbS_2$) and skinnerite (Cu_3SbS_3) along the Cu_2S - Sb_2S_3 join, famatinite (Cu_3SbS_4) along the hypothetical join of CuS - SbS and tetrahedrite ($Cu_{12+x}Sb_{4+y}S_{13}$), where $0 \leq x > 1.92$ and $-0.02 < y < 0.27$, as a phase without simple stoichiometry, as illustrated in Figure 17.

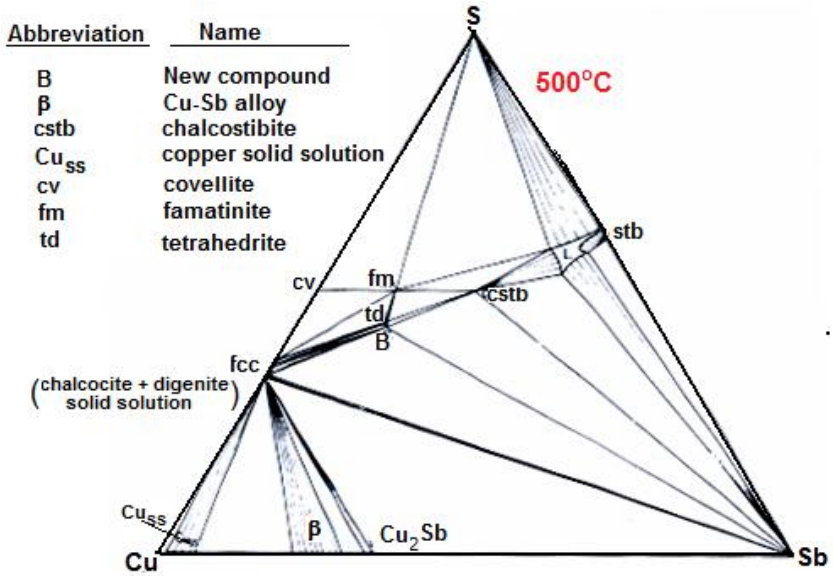

Figure 17. Phase relations in the Cu-Sb-S system at 500°C (element concentrations are in at. %) [91].

Sulfosalts have relatively fast rates of equilibration at T ≥ 400°C. Their structures are characterized by subunits similar to the component simple sulfides. The free energy of reaction, ΔG_m, that stabilizes the sulfosalts is relatively small (as shown in Figure 18), which is in agreement with Barton's et al. [92] conclusion: "for a given sulfosalt it is not a great deal to be more stable than any other alternative configurations representing the same bulk composition."

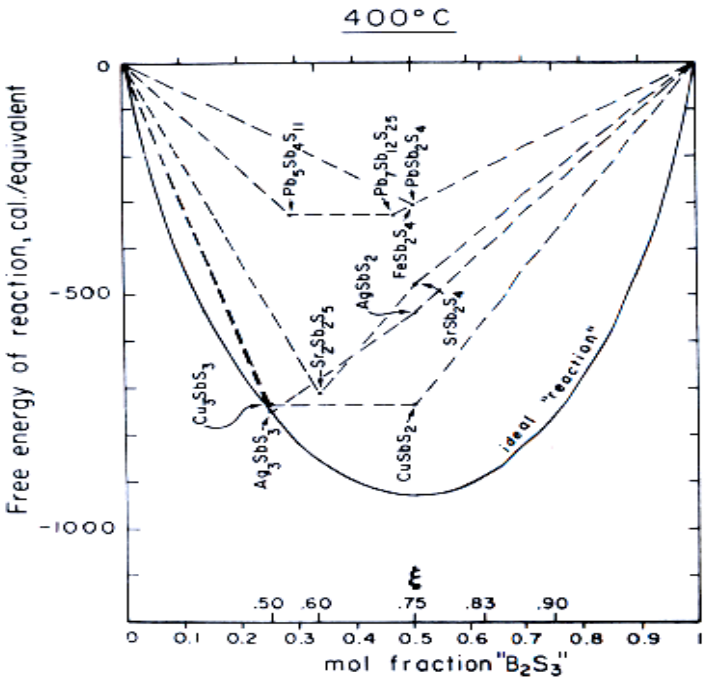

Figure 18. Free energies of reaction (= stabilization) of several sulfosalts at 400°C. Mole fractions are in terms of complete sulfide formula unit (i.e., AgS and Sb_2S_3) [86].

The calculation of the stabilizing energy is straight forward but requires knowledge of the relevant phase equilibria, the free energies of formation of the simple sulfides and the a_{S_2} in equilibrium with the univariant assemblage in question. For example, if we consider matildite ($AgBiS_2$) at 510°C, from the work of Craig et al. [93] we know that there exists a univariant assemblage which contains Ag_2S + $AgBiS_2$ + Bi-liquid + S_2 (g) (assumption was made on the effects of solid solution of Ag_2S in $AgBiS_2$ and the solubility of Ag and S in Bi(l) to be negligible – not quite true but the errors might be negligible) and then we can make use of the equilibrium $a_{S_2} = 10^{-6.73}$ atm from the work of Schenck et al. [94]. This assemblage is equivalent to reaction (9).

$$2/3Ag_2S + 4/3Bi + S_2\,(g) = 4/3\ AgBiS_2 \qquad (9)$$

$$\Delta G = -52891 + 34.34T \text{ (for T= 271....343°C)}$$

$$4/3Bi + S_2 = 2/3Bi_2S_3 \qquad (10)$$

If we treat the solids and Bi-liquid as invariant compositions (so that their activities are unity), the change in free energy of the reaction may be written as $\Delta G = - RT\ln(1/a_{S_2})$ which implies $\Delta G(510^\circ C)$ = - 24097cal.. $\Delta G(510^\circ C)$ for the reaction (10) is only - 21798 cal.. The difference between these two values represents the free energy which makes 4/3 mole of $AgBiS_2$ is more stable than a simple mixture of 2/3 mole of Ag_2S and 2/3 mole of Bi_2S_3. The free energy of formation of the phase $AgBiS_2$ from the elements at the same temperature is then merely the sum of the free energies of formation of ½Ag_2S + ½Bi_2S_3 + stabilizing energy.

"Any stable intermediate sulfosalt must be more stable than the combined end-members, i.e., free energy of the compound must be more negative than the appropriately weighed free energies of the end members," Craig et al. [86].

7.4 Stoichiometry of the Sulfides

Nonstoichiometry can be a very small fraction of atomic percent as in pyrite or very large as in $Fe_{1-x}S$ and $Ni_{1-x}S$. In either cases it manifests itself in the variables such as electrical, optical and chemical property of the minerals. The rigid definition of the term "polymorphism" requires that the high and low temperature forms have identical compositions. Because of nonstoichiometry this requirement is not often met by phases which are compositionally closely-related to one another. Scott et al. [73] recommended that definition of polymorphism to be relaxed to accommodate phases which are obviously related by composition but which exhibit a nonstoichiometric proportion of elements of one or two atomic percent.

The effect of nonstoichiometry on polymorphic inversions can be described by the Zn-S system, which shows an unusually wide range in inversion temperature with a_{S_2}. As mentioned in section 6.3.2, zinc sulfide is known to be nonstoichiometric, although the composition range is small. Allen et al. [95] proposed sphalerite to wurtzite transformation as follows:

ZnS (lower temperature cubic) (sphalerite) $\xrightarrow{1020^{o}C \text{ at } 1 \text{ atm}}$ ZnS (higher temperature hexagonal) (wurtzite)

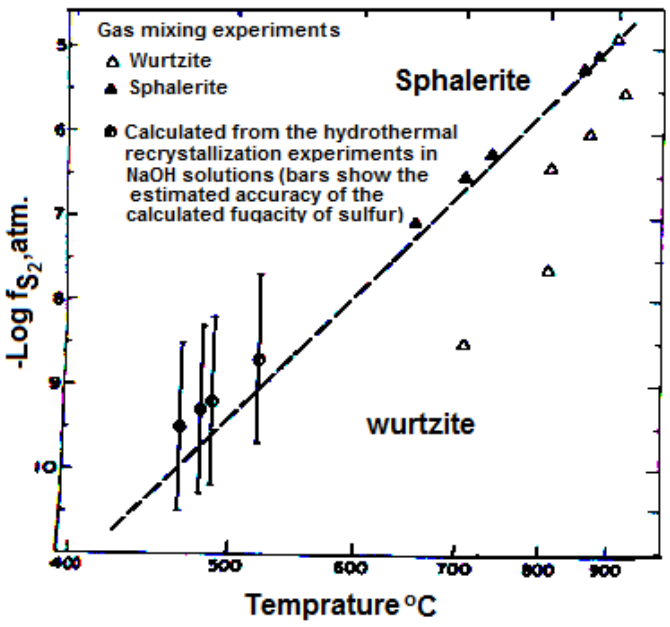

Figure 19. The univariant sphalerite-wurtzite boundary as a function of fugacity of sulfur and temperature at 1 atm. [73].

However, Scott et al. [73] have examined the sphalerite to wurtzite equilibrium by means of hydrothermal recrystalization and H_2/H_2S gas-mixing experiments in which f_{S_2} was controlled. Their

experiment, illustrated in Figure 18, showed that sphalerite and wurtzite can coexist over a range of temperature well below 1020°C as a function of f_{S_2}.

The f_{S_2}-dependence of the equilibrium requires that wurtzite is S-deficient relative to sphalerite. The effect of other elements in solid solution on the stability of wurtzite vs. sphalerite is largely unknown. However, there are evidences from unpublished experimental results that at 300°C and 400°C Cd-rich crystals have the wurtzite structure at values of f_{S_2} higher than that of the univariant curve in Figure 18 [1]. Fe substitution appears to have the opposite effect of stabilizing the sphalerite structure, at very low f_{S_2}. Barton et al. [75] found that Fe saturated zinc sulfide buffered by Fe + FeS to be sphalerite and not wurtzite at temperatures below 850°C.

8 Sulfide Petrology

In spite of the widespread occurrence of its minerals, sulfur is a minor constituent of the crust compared to the redox-participating elements such as iron, carbon, hydrogen and oxygen. Therefore, the latter elements are the one that ultimately exert the controlling influence on the activity of sulfur as well as on the mineralogy of sulfides.

Complexity of the problem of interpreting mineral associations originates from the unraveling of complex depositional pattern which may have been masked or erased by post-depositional processes. Investigations main goal is therefore to recognize and characterize equilibrium mineral assemblage groups of minerals that represent a current or former equilibrium state. Nonetheless, this is the most difficult and neglected part of sulfide mineralogy. With the exception of magnetic segregation, the processes of formation of most sulfide ores involve deposition from a dominantly aqueous solution. Sulfide ores tend to be depositories of the rarer elements. As a consequence of this and the chemical changes, the number of mineral species in a deposit as a whole can be large, sometimes much larger than it would be permitted by the phase rule. However, recent detailed studies inevitably reduces the mineralogical complexity to the extent that for any single stage of mineralization there are usually far too few, rather than too many, phases for the number of components.

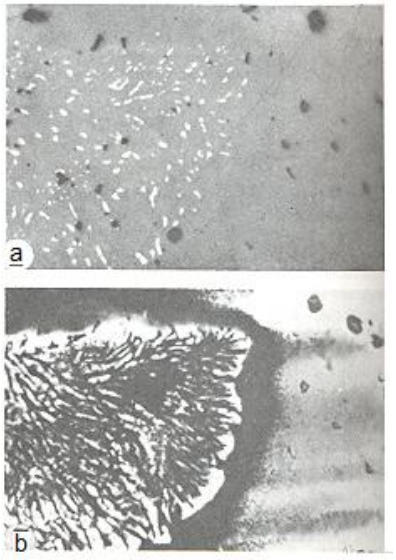

Figure 20. Growth-zoned sphalerite, the specimens were doubly polished sections thickness in the range 0.05 to 0.5mm. a) Reflected light (photo width: 0.25 mm) image b) transmitted light image [1].

The interpretation of ore textures is complex. Paul et al. [1] examined a standard polished section of a rock, as shown in Figure 20 (a) and (b). In a reflected light they observed a uniform field of sphalerite with a few blebs of chalcopyrite to one side, which seemed to be difficult to conclude

whether the chalcopyrite had grown with, exsolved from, replaced, or has been replaced by sphalerite. For the same site but illuminated with transmitted light (Figure 20 b) they proposed that the colorless sphalerite with chalcopyrite, replacing bonded yellow sphalerite, a feature that would never have been recognized in a normal examination of the polished section.

The second major aspect in petrology is the intervention of post depositional processes. For example, many sulfide deposits have been oxidized and subjected to supergene enrichment. Figure 21 shows the rates of reaction of sulfides to vary widely; however, they equilibrate faster than silicates and oxides.

Consequently, some sulfide minerals such as argentite (Ag_2S) or chalcopyrite may react internally to homogenize initial compositional zoning or reactions may occur between some sulfides while adjacent. More refractory sulfides such as sphalerite, pyrite or silicates are intact. Sulfide minerals are known to be affected by metamorphic effects even at a fine-scale that the record of their heritage is completely erased.

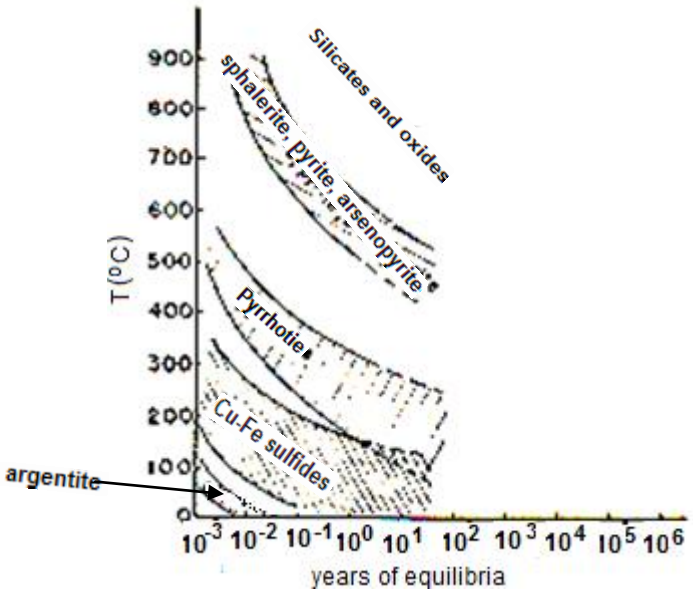

Figure 21. Time for equilibration for various minerals as a function of temperature [1].

8.1 Thermodynamic Approach

Many sulfidation reactions are too sluggish to obtain heats of reaction directly [1]. The best approach for sulfides appears to be to measure the equilibrium constant of formation of a phase at high temperatures and then to extrapolate to other temperatures using the heat content data and evaluation of activities, if solid solutions are involved.

Concluding the phase relations to be relatively insensitive to pressure of the magnitude found in the upper crust, Paul et al. [1] stressed on the effect of temperature and composition to be the most important. In addition, they identified the activity of sulfur to serve as a unifying unit of

different bulk composition. a_{S_2} is inversely proportional to the temperature, as shown in Figure 22 below.

The equation relating composition and activity of a component can be expressed as:

$$X = \frac{\text{a(composition, temperature and pressure of the environment)}}{\gamma\text{(composition, temperature and pressure of the growing crystal)}} \quad (12)$$

where γ is activity coefficient. Activity can be locally buffered or it may be controlled remotely, as a_{NiS} might be controlled through the interaction of H_2S - bearing fluids with nickel-bearing silicates far removed from the site of deposition. The solubility of sulfur in basaltic melts is controlled strongly by the activity of FeS which in turn is controlled by the activity of sulfur and oxygen, and to a lesser extent by CaO.

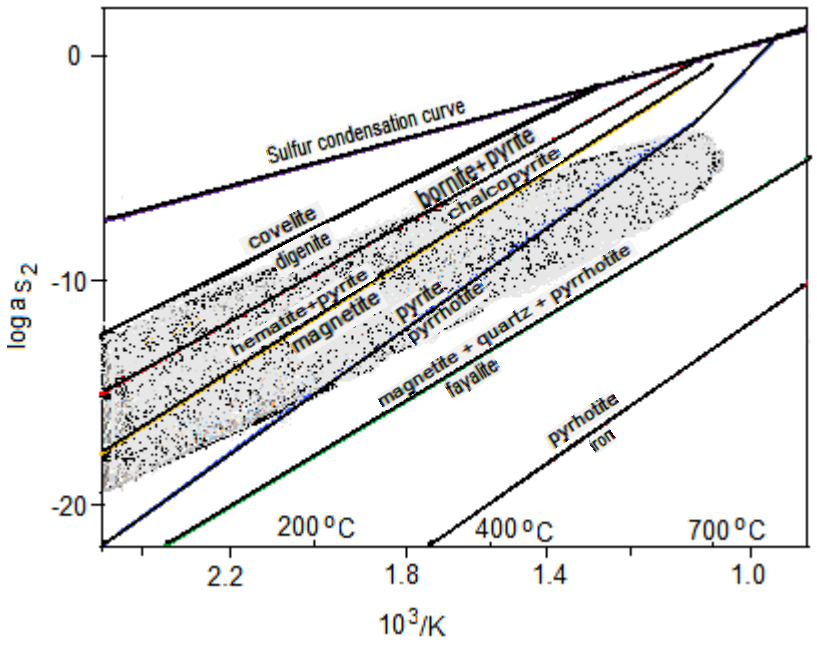

Figure 22. Log$\mathbf{a_{S_2}}$ vs. T diagram showing typical sulfidation reactions and region of principal ore-forming environments. The shaded region indicating the "main line" of ore-forming environment [1].

The metallogenic diagram of sulfidation reactions shown in Figure 22 covers a large range of sulfur activities, and some deposits may have sufficient mineralogical variation to be represented by one-third or more of the total a_{S_2} range.

"Despite the essential non-existence of a molecular sulfur species in the ore forming environment, the activity of sulfur (a_{S_2}) is extremely useful because it relates different sulfide assemblages to a common variable that exerts a significant control over sulfide mineralogy," Paul et al. [1].

9 Summary and Conclusions

Most of the transition metal sulfides assume the NiAs-type structure (shown in appendix A). Non-stoichiometry (usually metal atom vacancies) and derivative structures are also very common. The sulfosalts may be described as the sphalerite-type structure (shown in appendix A) by omission of the forth S. Sulfides extensively exhibit polymorphism; the well known polymorphs marcasite and pyrite belong to these materials system. The relationships between troilite (FeS) and the pyrrhotites ($Fe_{1-x}S$) are also structural rationalization, which vaguely described as non-stoichiometry.

The crystal chemistry, thermochemistry and phase equilibria of the metal sulfides discussed are connected with the relatively pure materials which are observed mainly as synthetic phases. Natural sulfides normally contain impurities, and natural assemblages are frequently more complex than those studied in laboratory experiments. Differences between natural and synthetic sulfides may or may not have a significant effect on some properties, and studies to contain effects of the impurities are crucial aspects of the sulfides research.

The experimental studies of the sulfides involve synthesis and analysis of the synthesized sulfides. Due to its non reactivity with sulfur, stability at elevated temperatures (up to 1100 ^{o}C) and good resistance to thermal shock fused silica is a widely used material for sulfides synthesis. Analysis of the obtained products by microscopy, X-ray diffractometry and microprobe analysis and others lead to the conventional graphical representation. Such studies, prior to the year 1975, were somehow suppressed by the accuracy of the times technology. For instance, the X-ray examination to determine the crystal structures of sulfosalts was often encountered high radiation absorption by the heavy metal atoms like Pb and Bi. Metastable phase formations and their survival of equilibrium tests and non-quenchability nature of some phases were also great sources of error.

Results of the experiments can be presented diagrammatically in a number of ways depending on the variables measured. The most commonly used are T-X and $\log a_{S_2}$-10^3/T plots. The significance of the later relation could have arisen from the fact that many sulfide reactions can be expressed as a sulfidation of one solid to another. It also appeared to be a standard means of presenting sulfidation reactions as well as sulfide petrogenetic grids.

Most sulfosalts can be regarded as intermediate phases on joins between simple sulfides and they are thermodynamically favored than any other alternative configurations representing the same bulk composition. The temperature and activity of sulfur are the main controlling thermodynamic variables of the sulfides phase transformation and formation of assemblages. Sulfides equilibrate faster than the silicates and oxides, on the geological time scale, and often affected by the metamorphism which makes the determination of ore genesis complex.

Acknowledgements

The authors are grateful to Improved Sulfide Smelting (ISS) project of the ELEMET program and Tekes, the Finnish Funding Agency for Technology and Innovation, for financial support. This work was made as a sub task of ISS, supported financially by Boliden Harjavalta Oy, Boliden Kokkola Oy, Norilsk Nickel Finland Oy and Outotec Oyj.

Reference

1. Wuensch, B.J., Rajamani, V., Prewitt, C.T., Scott, S.D., Craig, J.R. and Barton, P.B. Sulfide Mineralogy. Mineralogical Society of America, Short Course Notes. 1974. 281 p.
2. Kullerud, G. The FeS-ZnS System, a Geological Thermometer. Norsk Geol. Tiddsskr. 32. 1953. pp. 61-147.
3. Rosenqvist, T. A Thermodynamic Study of the Iron, Cobalt and Nickel Sulfides. J. Iron Steel Inst. 176. 1954. pp. 37 - 57.
4. Toulmin, P. and Barton, P.B. A Thermodynamic Study of Pyrite and Pyrrhotite. Geochim. Cosmochim. Acta, 28. 1964. pp. 641-671.
5. Evans, H.T. Crytal Structure of Low Chalcocite. Nature 232. 1971. pp. 29 – 70.
6. Welin, E. Notes on the Mineralogy of Sweden S. Bismuth-bearing Sulphosalts from Gladhammar, a Revision. Ark. Mineral. Geol. 4. 1966. pp. 377-386.
7. Pauling, L. and Neumann, E.W. The Crystal Structure of Binnite (Cu, Fe)$_{12}$As$_4$S$_{13}$, and the Chemical Composition and Structure of Minerals of the Tetrahedrite group. Z. kristallogr. 88. 1934. pp. 54-62.
8. Skinner, B.J. The Pseudobinary System Cu_2FeSnS_4-Cu_2ZnSuS_4 and Its Mineralogical Significance. Can. Mineral. Mag. 37. 1972. pp. 535-541.
9. Tatsuka, K. and Morimoto, N. Composition Variation and Polymorphism of Tetrahedrite in the Cu-Sb-S System Below 400^{o}C. Am. Mineral. 58.1973. pp. 425-434.
10. Donohue, Jerry, Aimery, C., Elihu, G. The Crystal Molecular Structure of S_6 (Sulfure-6). J. Am. Chem. Soc. 83. 1961. pp. 3748 - 3751.
11. Marumo, F. The Crystal Structure of Nawackiite, $Cu_6Zn_3AsS_{12}$. Z. Kristalogr. 124. 1967. pp. 352 – 368.
12. Evans, H.T. Lunar Troilite: Chrystalography. Science 167. 1970. pp. 621-623.
13. Hall, S. R. and Stewart, J. M. The Crystal Structure of Argentian Pentlandite (FeNi)$_8$AgS$_8$, Compared with the Refined Structure of Pentlandite (Fe, Ni)$_9$S$_8$. Can. Mineral. 12. 1973. pp. 169-177.
14. Takagi, J. and Takeuchi, Y. The Crystal Structure of Lillianite ($Pb_3Bi_2S_6$). Acta Crystallogr. B28. 1972. pp. 649 – 651.
15. Weitz, G. and Hellner, E. Über Komplex Zusammengesetzite Sulfidische Erze VII. Zur Kristallstruktur Des Cosalits, $Pb_2Bi_2S_5$. Z. Kristallogr. 113. 1960. pp. 385 – 402.

16. Kupcik, V. and Makovicky, E. Die Kristallstruktur Des Minerals (Pb, Ag, Bi)$Cu_4Bi_5S_{11}$. Neues Jahrb. Mineral. Monnatsh. 1968. pp. 236 – 237.

17. Ohmassa, Masaaki and Nowacki, W. The Crystal Structure of Synthetic CuBi5S8. Z. Kristallogr. 137. 1973. pp. 422- 432.

18. Kohatsu, Iwao and Wuensch, B. J. The Crystal Structure of Gladite, $PbCuBi_5S_9$ (abstract). Am. Minral. 58. 1973b . 1098 p.

19. Kohatsu, Iwao and Wuensch, B. J. The Crystal Structure of Nuffieldite, $Pb_2Cu(Pb,Bi)Bi_2S_7$. Z. Kristallogr. 1973a. pp. 343 – 365.

20. Rajamani, V. and Prewitt, C. T. The Crystal Structure of Millerite. Can. Mineral. 12. 1974a. pp. 235 – 257.

21. Rajamani, V. and Prewitt, C. T. Thernmal Expansion of Pentlandite Structure. Am. Mineral. (in press). 1974b.

22. Rajamani, V. and Prewitt, C. T. Crystal Chemistry of Natural Pentlandites. Can. Mineral. 12. 1973. pp. 178 – 187.

23. Taylor, L. A. and Finger, L. W. Structure Refinement and Composition. Carnegie Inst. wash. Year Book, 69. 1971. pp. 319 – 323.

24. Geller, S. Refinement of the Crystal Structure of Co_9S_8. Acta Crystallogr. 15. 1962. pp. 1195 – 1198.

25. Fleet, M. E. The Crystal Structure of α-Ni_7S_6. Acta Crystallogr. B28. 1972. pp. 1237 – 1241.

26. Nickel, E. H. The Application of Ligand Field Concepts to an Understanding of the Structural Stabilities and Solid Solution Limits of Sulfides and Related Minerals. Chem. Geol. 1970. pp. 233 – 241.

27. Knop, O. and Ibrahim, M. A. Chalcogenides of the Transition Elements. II. Existence of the π Phase in the M9S8 Section of the System Fe-Co-Ni-S. Can. J. Chem. 39. 1961. pp. 297 – 317.

28. Vaughan, D. J., Burns, R. J. and Burns, V. M. Geochemistry and Bonding of Thiospinel Minerals. Geochim. Cosmochim. Acta 35. 1971. pp. 365 – 381.

29. Lewis, G. N. and Radall, M. Thermodynamics. 2nd edition. Revised by Pitzer, K. S. and Brewer, L., McGraw-Hill, Inc., New York. 1961.

30. Taylor, L. A. Low-Temperature Phases Relations in the Fe-S System. Carnegie Inst. Wash. Year Book. 1970a. pp. 259 – 270.

31. Kissin, S. A. Phase Relation in a Portion of the Fe-S System. Ph. D. Thesis. University of Toronto. 1974.

32. Kullerud, G. Experimental Techniques in Dry Sulfide Research. In , Ulmer, G. C., Ed., Research Techniques for High Pressure and High Temprature. Springer- Verlag, New York. 1971. pp. 288 – 315.

33. Moh, G. H. and Taylor, L. A. Laboratory Techniques in Experimental Petrology. Neues Jahrb. Miner. Monatsh. 1971. pp. 450 – 459.

34. Barnes, H. L. Investigations in Hydrothermal Sulfide Systems. In, Ulmer, G.C., Ed., Research Techniques for High Pressure and High Temperature. Springer-Verlag, New York. 1971. pp. 317 – 355.

35. Barnes, H. L. and Czamanske, G. K. Solubilities and Transport of Ore Minerals. In, Barnes, H. L., Ed., Geochemistry of Hydrothermal Ore Deposits. Holt, Rinehart, and Winston, New York. 1967. pp. 334 - 381.

36. Kissin, S. A. and Scott, S. D. Phase Relations of Intermediate Pyrrhotites (abstract). Econ. Geol. 67. 1972. 1007 p.

37. Barton, P. B. and Skinner, B. J. Sulfide Minerals Stabilities. In, Barnes, H. L., Ed., Geochemistry of Hydrothermal Ore Deposits. Holt, Rinehart and Winston, Inc., New York. 1967. pp. 236 – 333.

38. Braune, H., Peter, S. and Neveling, V. Die Dissoziation des Schwefeldsampfes. Z. Naturforsch. 62. pp. 32 – 37. 1951.

39. Mills, K. C. Thermodynamic Data for Inorganic Sulphides, Selerides, and Tellurides. Butterworths, Loondon. 1974. 845 p.

40. Schneeberg, E. P. Sulfur Fugacity Measurements with the Electrochemical Cell Ag|AgI|$Ag_{2+x}S$, $fS_2(g)$. Econ. Geol. 68. 1973. pp. 507 – 517.

41. Sato, M. Electrochemical Measurements and Control of Oxygen Fugacity and Other Gaseous Fugacities with Solid Electrolyte Sensors. In, Ultmer, G. C., Ed., Research Techniques for High Pressure and High Temprature. Springer- Verlag, New York. 1971. pp. 43 – 99.

42. Craig, J. R., Skinner, B. J., Francis, C. A., Luce, F. D., Makovicky, E. Phase Relations in the As-Sb-S System. Trans. Am. Geophys. Union 55. 1974. 483 p.

43. Ehlers, E. G. The Interpretation of Geological Phase Diagrams. Freeman, W. H. and Co., San Fransisco. 1972. 280 p.

44. Gronvold, F. and Haraldsen, H. On the Phase Relations of Synthetic and Natural Pyrrhotites. Acta Chem. Scand. 6. 1952. pp. 1452 – 1469.

45. Yund, R. A. and Hall, H.T. The Miscibility Gap between FeS and Fe1-xS. Mat. Res. Bull. 3. 1968. pp. 779 - 784.

46. Berner, R. A. Iron sulfides Formed from Aqueous Solution at Low Temperatures and Atmospheric Pressure. J. Geol. 72. 1964. pp. 293 – 306.

47. Takeno, S. and Clark, A. H. Observations on Tetragonal (Fe, Ni, Co)$_{1+x}$S, Mackinawite. J. Sci. Hiroshima Univ., Ser. C. 5. 1967. pp. 287 – 293.

48. Zoka, H., Taylor, L. A., Takeno, S. Compositional Variations in Natural Mackinawite and the Results of Heating Experiments. J. Sci. Hiroshima Univ., Ser. C, 7. 1973. pp. 37 – 53.

49. Nakazawa, H. and Morimoto, N. Phase Relations and Superstructures of Pyrrhotite, $Fe_{1-x}S$. Mater. Res. Bull. 6. 1971. pp. 345 – 358.

50. Corlett, M. Low-Iron Polymorphs in the Pyrrhotite Group. Z. Kristallogr. 126. 1968. pp. 124 – 134.

51. Desborough, G. A. and Carpenter, R. H. Phase Relations of Pyrrhotite. Econ. Geol. 60. 1965. pp. 1431 – 1450.

52. Byström, A. Monoclinic Magnetic Pyrites. Ark. Kemi Mineral. Geol. 19B. 1945. pp. 1 -8.

53. Clark, A. H. Stability Field of Monoclinic Pyrrhotite. Inst. Min. Metal. Trans. 75B. 1966. pp. 232 – 235.

54. Arnold, R. G. Pyrrhotite Phase Relations Below 304 ± 6°C at < 1 atm Total Pressure. Econ. Geol. 64. 1969. pp. 405 – 419.

55. Yund, R. A. and Hall, H.T. Hexagonal and Monoclinic Pyrrhotites. Econ. Geol 64. 1969. pp. 420 - 423.

56. Yund, R. A. and Hall, H.T. Kinetics and Mechanism of Pyrite Exsolution from Pyrrhotite. J. Petrol. 11. 1970. pp. 381 - 404.

57. Rising, B.A. Phase Relations among Pyrite, Marcasite and Pyrrhotite Below 300°C. Ph.D Thesis, Pennsylvania State University. 1973.

58. Yamaguchi, S. and Wada, H. Fe_2S_3 of the Spinel Type Structure with Lattice Defect. Kristall und Technik, 8. 1973. pp. 1017 - 1019.

59. Erd, R. C., Evans, H. T. Jr. and Richter, D. H. Smthite, a New Iron Sulfide and Assicited Pyrrhotite from Indiana. Am. Mineral. 42. 1957. pp. 309 – 333.

60. Kullerud, G. Sulfide Studies. In, P. H. Abelson, Ed., Researches in Geochemistry, vol. 2. John Wiley and Sons. 1967. pp. 286 – 321.

61. Taylor, L. A. and Williams, K. L. Smythite, $(Fe, Ni)_9S_{11}$ – a Redefinition. Am. Mineral. 57. 1972. pp. 1571 – 1577.

62. Nickel, E. H. Nickelferous Smythite from Some Canadian Occurences. Can. Mineral. 11. 1972. pp. 514 – 519.

63. Bennett, C. E. G., Graham, J. and Thornber, M. R. New Observation on Natural Pyrrhotites. Part I – Mineragraphic Techniques. Am. Mineral. 57. 1972. pp. 445 – 462.

64. Rickard, D. T. Synthesis of Smythite- Rhombohedral Fe_3S_4. Nature 218. 1968. 356 p.

65. Roseboom, E.-H. An Investigation of the System Cu-S and Some Natural copper Sulfides Between 25°C and 700°C. Econ. Geol. 61.1966. pp. 641 – 672.

66. Morimoto, N. and Koto, K. Phase Relations of the Cu – S System at Low Temperature: Stability of Anilite. Am. Mineral. 55. 1970. pp. 106 – 117.

67. Barton, P. B., Jr. Solid Solutions in System Cu-Fe-S Part I. The Cu-S and CuFe-S Joins. Econ. Geol. 68. 1973. pp. 455 – 465.

68. Morimoto, N. and Kullerud, G. Polymorphism in Digenite. Am. Mineral. 48. 1963. pp. 110 – 123.

69. Evans, H. T., Jr. A Crystal Structure Study of Low Chaococite (abstract). Geol. Soc. Am. Abstr. Programs 92. 1968.

70. Skinner, Brian J. Stability of the Tetragonal Polymorph of Cu_2S. Econ. Geol. 65. 1970. pp. 727 – 730.

71. Serebryanaya, N. R. On the Tetragonal Modification of Chalcocite. Geochem. Int. 3. 1966. pp. 687 – 688.

72. Arnold, R. G. and Malik, O. P. The NiS-S System Above 980^{o}C – A Revision. Econ. Geol. (in press). 1974.

73. Scott, S. D. and Barnes, H. L. Sphalerite-Wurtzite Equilibria and Stoichiometry. Geochim. Cosmochim. Acta 36. 1972. pp. 1275 – 1295.

74. Scott, S. D. and Barnes, H. L. Sphalerite Geothermometry and Geobarometry. Econ. Geol. 66. 1971. pp. 653 – 669.

75. Barton, P. B., Jr. and Toulmin, P. Phase Relations Involving Sphalerite in the Fe-Zn-S System. Econ. Geol. 61. 1966. pp. 815 – 849.

76. Manning, P. G. Absorption Spectra of Fe (III) in Octahedral Sites in Sphalerite. Can. Mineral. 9. 1967. pp. 57 – 64.

77. Cabri, J.L. New Data on Phase Relations in the Cu-Fe-S System. Econ. Geol. 68. 1973. pp. 443 – 454.

78. Kullerud, G. The Fe-Ni-S System. Carnegie Inst. Wash. Year Book, 62. 1963. pp. 175 – 189.

79. Bell, P. M., England, J. L. and Kullerud, G. Pentlandite: Pressure Effect on Breakdown. Carnegie Inst. Wash. Year Book 64. 1964. pp. 206 – 207.

80. Vaasjoki, O., Hakli, T. A. and Tonitti, M. The Effect of Cobalt on the Thermal Stability of Pentlandite. Econ. Geol. 69. 1974. pp. 549 – 551.

81. Scott, S. D. Mössbauer Spectra of Synthetic Iron-Bearing Sphalerite. Can. Mineral. 10. 1971. pp. 882 – 885.

82. Scott, S. D. and Kissin, S. A. Sphalerite Composition in the Zn-Fe-S System Below 300^{o}C. Econ. Geol. 68. 1973. pp. 475 – 479.

83. Kullerud, G., Yund, R. A. and Moh, G. H. Phase Relasions in the Cu-Fe-S System. In, Wilson, H.D.B., Ed., Magmatic Ore Deposits, Econ. Geol. Monogr. 4. 1969. pp. 323 - 343.

84. Wang, H. Kinetic Studies of Some Solid-State Reactions of Metal Sulfides. PhD Thesis. University of Adelade, School of Chemical Engineering. 2005. 126 p.

85. Morimoto, N. and Kullerud, G. Pentlandite: Thermal Expansion. Carnegie Inst. Wash. Year Book 64. 1965. pp. 204 – 205.

86. Craig, J. R. and Barton, P. B. Thermochemical Approximations for Sulfosalts. Econ. Geol. 68. 1973. pp. 493 – 506.

87. Takeuchi, Y. On the Crystal Chemistry of Sulphides and Sulphosalts. In, volcanism and Ore Genesis, Ed., Tatsumi, T., Univ. Tokyo Press. 1970. pp. 395 – 419.

88. Hellner, E. A Structural Scheme for Sulfide Minerals. J. Geol. 66. 1958. pp. 503 – 525.

89. Nowacki, W. Zur Klassifikation und Kristallchemie der Sulfosalze. Schweiz. Mineral. Petrogr. Matt. 49. 1969. pp. 109 – 156.

90. Takeuchi, Y. and Sadanaga, R. Structural Principles and Classification of Sulfosalts. Z. Kristallogr. 130. 1969. pp. 346 – 368.

91. Skinner, Brian J., Luce, Fredrick D. and Makovicky, Emil. Studies of the Sulfosalts of Copper III. Phases and Phase Relations in the System Cu-Sb-S. Econ. Geol. 67. 1972. pp. 924 – 938.

92. Barton, P. B. Jr. Thermochemical Study of the System Fe-AS-S. Geochim. Cosmochim. Acta, 33. 1969. pp. 841 – 857.

93. Craig, J. R., Cubicciotti, D. The Bismuth – Sulfur Phase Diagram. J. Phys. Chem. 66. 1962. pp. 1205 – 1206.

94. Schenck, R. and Von der Forst, P. Gleichgewichtsstudien an Erzbildenchen Sulfiden II. Z. anorg. Chem. 2H. 1939. pp. 145 – 157.

95. Allen, E. T. and Crenshaw, J. L. The Sulfides of Zinc, Cadmium, and Mercury; Their Crystaline Forms and Genetic Conditions. Am. J. Sci. Ser. 4, 34. 1912. pp. 341 – 396.

96. Scott, S.D. Mössbauer Spectra of Synthetic Iron-Bearing Sphalerite. Can. Mineral. 10 . 1971. pp. 882-885.

Appendix A

Some of the typical unit cells of the most common sulfides of the transition metals.

Name	Crystal structure
NiAs structure type	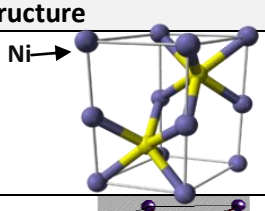
CdI_2-type layer structure	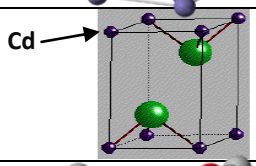
Marcasite(FeS_2)	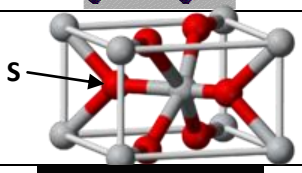 S-S= 2.21Å
Pyrite(FeS_2)	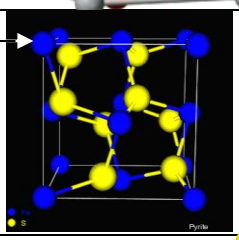 S-S= 2.21Å
(ZnS) - Sphalerite/zinc blende (left) and Wurtzite (right)	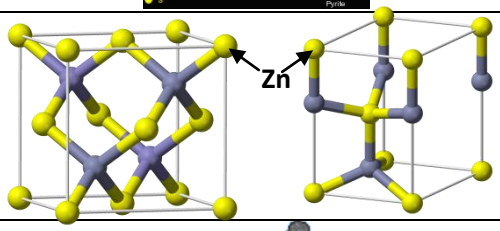
As_4S_4	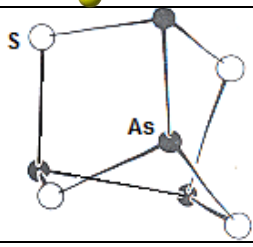
FeAsS	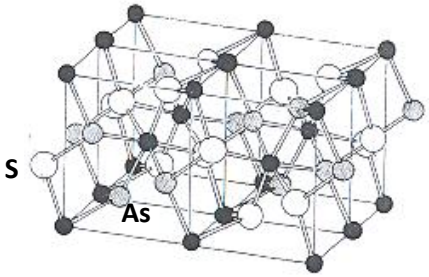
PtS	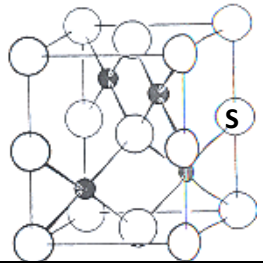

Appendix B

Schematic isothermal sections of the condensed FeS-ZnS-S system showing the extensive solid solution of FeS in ZnS and its dependence on the Fe-sulfide(s) coexisting with sphalerite [96].

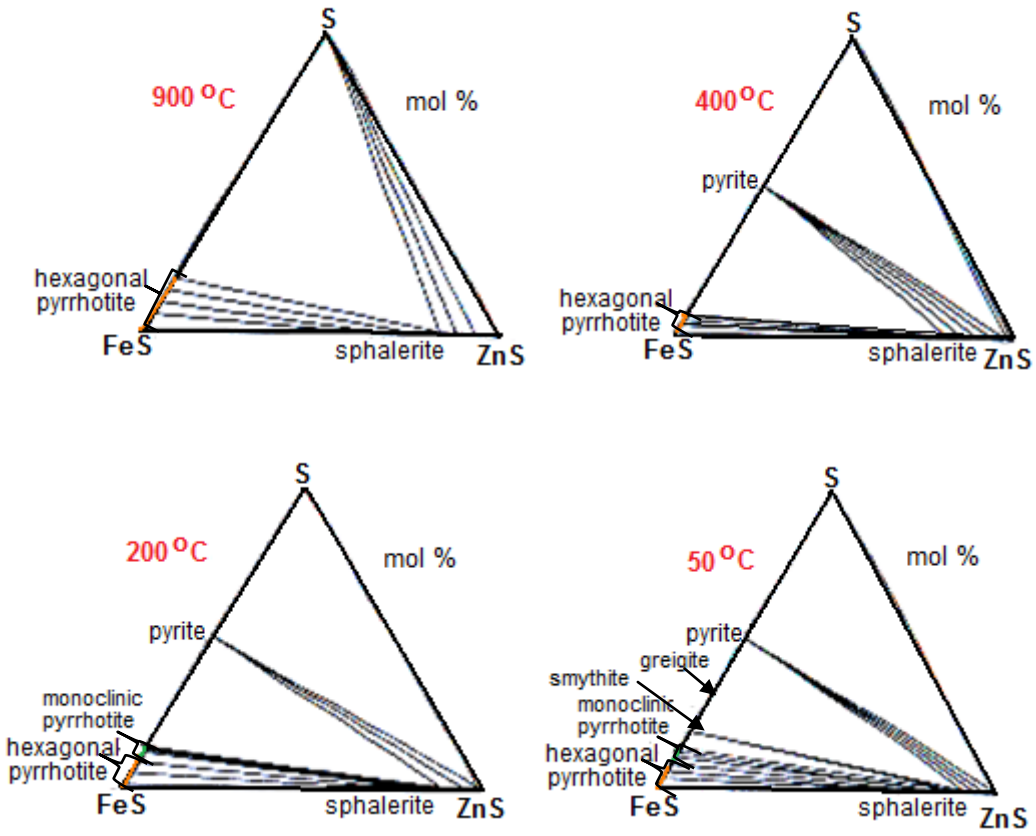

HELSINKI UNIVERSITY OF TECHNOLOGY PUBLICATIONS IN MATERIALS SCIENCE AND ENGINEERING

TKK-MT-200 Aromaa, J., Galfi, I., Karonen, M., Schmachtel, S., Suntio, A.
Corrosion of Copper in Ground Water Vapour. 2008

TKK-MT-201 Heikinheimo,E.,Selin,L.,(ed.),
Possibilities of electron excited microbeam analysis in materials science. Graduated School Seminar, 2008 at TKK, Espoo, Finland

TKK-MT-202 Miettinen, J.,
Tentative thermodynamic description of ternary Fe-Mo-B, Fe-Nb-B, Fe-Ti-B and Fe-V-B systems. 2008

TKK-MT-203 Kekkonen, M. (ed.),
Materials production and synthesis / 2008

TKK-MT-204 Heikinheimo, E., Selin, L. (editors),
Defect Structure and Reactivity of Solids. 2009

TKK-MT-205 Miettinen, J.,
Thermodynamic description of the Fe-Nb-Ti-V-C-N system. 2009

TKK-MT-206 Miettinen, J., Kytönen, H.,
Thermodynamic descriptions of Fe-Mn-Si, Fe-Mn-B and Fe-Si-B systems. 2009

TKK-MT-207 Huitu, K., Kekkonen, M., Holappa, L.,
Novel Steelmaking Processes. 2009

TKK-MT-208 Bunjaku, A., Holappa, L.,
Thermodynamic properties of NICKEL laterite ores. 2009

TKK-MT-209 Heikinheimo, E., Selin, L. (editors),
Quantitative electron probe microanalysis in materials science.
Graduate School Seminar, September 25, 2009 at TKK, Espoo, Finland

TKK-MT-210 Keski-Honkola A., Vaajoki, A., Oksanen, J., Hämäläinen, M.,
Ag-Bi-Cu-Sn seoksen termodynaaminen mallintaminen FactSage-ohjelmalla. 2009

TKK-MT-211 Kekkonen, M., (ed.),
Materials Production and Synthesis / 2009 MT-0.3201

TKK-MT-212 Isomäki, I., Hämäläinen, M., Pirso, J., Ferreira, J., Braga, H.
Thermodynamic and Structural Study of Quaternary Ni-rich Fe-Ni-Ti-W Phase Diagram. 2009

TKK-MT-213 Heikinheimo, E., (ed.),
Activity Report 2007 – 2009. Department of Materials Science and Engineering. 2010

ISBN 978 952-60-3271-9
ISSN 1455-2329